CREB determines the expression of ST2 in T_{regs} and mediates the balance between type 1 and type 2 immune responses

Short title: T_{regs} require CREB to suppress ST2 expression

Sudheendra Hebbar Subramanyam[1], Judit Hriczko[1], Saskia Schulz[1], Thomas Look[2,3], Tannaz Goodarzi[1], Tim Clarner[4], Miriam Scheld[4], Markus Kipp[5], Eva Verjans[1], Svenja Böll[1], Christopher Neullens[1], Ivan Costa[6], Zhijian Li[6], Lin Gan[7], Bernd Denecke[7#], Angela Schippers[1], Stefan Floess[8], Jochen Huehn[8], Edgar Schmitt[9], Tobias Bopp[9], Hermann Wasmuth[10], Ron Winograd[10], Rudi Beyaert[11,12], Bart Lambrecht[11,13], Peter Boor[14], Martin Zenke[2,3], Norbert Wagner[1], Kim Ohl[1, §], Klaus Tenbrock[1, 15§*]

[1]Dept. of Pediatrics, RWTH Aachen University

[2]Institute for Biomedical Engineering, Department of Cell Biology, RWTH Aachen, University Hospital, Aachen, Germany

[3] Helmholtz Institute for Biomedical Engineering, RWTH Aachen University, Aachen, Germany.

[4]Institute of Neuroanatomy and JARA-BRAIN, Faculty of Medicine, RWTH Aachen University

[5]Institute of Anatomy, Medical University of Rostock, Rostock, Germany

[6]Instutute for Computational Genomics, IZKF, RWTH Aachen University

[7]Genomics Facility, Interdisciplinary Center for Clinical Research Aachen (IZKF Aachen), RWTH Aachen University, Aachen, Germany

[8]Department of Experimental Immunology, Helmholtz Centre for Infection Research, Braunschweig, Germany

[9]Institute for Immunology, University Medical Center, Johannes Gutenberg University Mainz, Mainz, Germany

[10]Luiusenhospital Aachen, Dept. of Medicine, Aachen, Germany

[11]VIB Center for Inflammation Research, Ghent, Belgium

[12]Department of Biomedical Molecular Biology, Ghent University, Ghent, Belgium

[13]Department of Respiratory Medicine, Ghent University Hospital, Ghent, Belgium

[14]Institute of Pathology, RWTH Aachen, University Hospital, Aachen, Germany

[15]Division of Pediatric Rheumatology, Department of Pediatrics, Inselspital, Bern University Hospital, University of Bern, Switzerland

§equal contribution

*Corresponding author: Klaus Tenbrock, Dept. of Pediatrics, RWTH Aachen University, Pauwelsstraße 30, 52074 Aachen, ktenbrock@ukaachen.de, 0049-2418089140

#Bernd Denecke unfortunately passed away during the project

Abstract

Regulatory T cells (T_{regs}) are gatekeepers of immune homeostasis and characterized by expression of Foxp3, which maintains T_{reg} identity. The cAMP response element binding protein CREB binds the TSDR and influences Foxp3 expression. To understand the functional consequences, we generated mice with a Foxp3-specific knockout of CREB. CREB deficient T_{regs} expand *in vivo* but show a reduced Foxp3 expression combined with an enhanced expression of IL-5, IL-13, IL-10, ST2 and CREM. This renders such T_{regs} highly suppressive *in vitro* and prevents disease activity in the Th1 model of T cell mediated transfer colitis in an IL-10 dependent way while it enhanced ovalbumin mediated asthma severity. While TSDR methylation was unchanged in CREB deficient T_{regs}, CREB and CREM directly interact with Foxp3 and deficiency of CREB alters chromatin accessibility at the IL13 and ST2 locus. Additional genetic CREM deficiency reverses the ST2 phenotype. Our data suggest that CREB expression in T_{regs} is important for the regulation of ST2 mediated balance between type 1 and type 2 immune responses.

Introduction

Regulatory T cells (T_{regs}) are important for the maintenance of immune homeostasis and characterized by expression of Foxp3. Loss of Foxp3 results in a devastating autoimmune syndrome in mice (scurfy disease)[1] and humans (IPEX, polyglandular autoimmunopathy)[2]. Two sources of Foxp3$^+$ cells have been described, one of which located to the thymus ("thymus-derived T_{regs}"; tT_{regs}), and the second to the periphery, where conventional CD4$^+$ T cells can convert into Foxp3$^+$ "inducible T_{reg}" cells (iT_{regs}) after T cell stimulation in the presence of TGF-β [3]. tT_{reg}-cell as well as iT_{reg} cell generation largely depend on the presence of IL-2 which is not only required for homeostatic maintenance but also for the thymic development of T_{reg} cells [4, 5, 6, 7].

The accessibility of the *Foxp3* gene promoter, as well as other cis-regulatory elements in the *Foxp3* locus are under tight epigenetic control, especially by histone acetylation, methylation and cytosine-phospho-guanosine (CpG-)DNA methylation [8] in particular at the Treg-specific de-methylated region (TSDR) [9, 10, 11]. The TSDR possesses transcriptional binding sites for the cAMP responsive element binding protein/activating transcription factor (CREB/ATF) [10, 11, 12] and CREB was identified as a positive regulator of Foxp3 expression *in vitro*.

Previous data from Wang et al. group suggested that CREB negatively regulates the survival of iTreg cells and is particularly important in the generation of CD4+ Th17 cells. Using CD4^{CRE} CREB$^{fl/fl}$ mice, they showed that these cells prevented colitis in a Rag2-/- model, however their model has the disadvantage that CD4 cells of these mice are expressing lower amounts of IL-2 that could even hamper iTreg induction. Our analysis now expands their findings and determines an important role for CREB in the generation of ST2 positive TRegs. Using Foxp3^{CRE} CREB$^{fl/fl}$ mice we herein confirm the colitis phenotype but can show that i) CREB deficiency in T_{regs} induces expression of ST2 positive T_{regs} associated with enhanced experimental asthma severity ii) the phenotype that prevents colitis in RAG mice is primarily dependent on abundance of IL-10, iii) and that this phenotype can be reversed by knockout of CREM that lowers expression of ST2.

Material and Methods:

Mice strains

Experiments were performed with age matched *CREB*$^{fl/fl}$, *Foxp3*^{cre}*CREB*$^{fl/fl}$ and *VAV*^{cre}*CREB*$^{fl/fl}$ mice (all C57BL/6). *Foxp3*^{cre}*CREB*$^{fl/fl}$ mice were generated by crossing CREB-flox mice [36] with C57BL/6 Foxp3-IRES Cre mice (provided by T. Bopp, University of Mainz). *Foxp3*^{cre}-*CREB*$^{fl/fl}$ mice were used as controls (denoted as *CREB*$^{fl/fl}$). *Foxp3*^{CRE}*ROSA*^{RFP} were were provided by T. Bopp University of Mainz and crossed with our *CREB*$^{fl/fl}$ mice. CD45.1 congenic mice (C57BL/6) and RAG$^{-/-}$ (C57BL/6) mice were provided by O. Pabst und A. Schippers. All mice were bred in our animal facility and kept under standardized conditions.

Mixed bone marrow chimeras

BM cells were isolated from femurs and tibias of age-matched donor animals (WT CD45.1 and *Foxp3*^{cre}*CREB*$^{fl/fl}$ CD45.2). RAG2$^{-/-}$ mice were lethally irradiated (2 x 6.8 Gy) and i.v. injected with 5 x 10^6 cells of each genotype after irradiation. The mice received antibiotic treatment for 14 days (40 µl Borgal-solution (24%) / 100 mL drinking water). Seven weeks later, the mice were sacrificed, and spleens analyzed by flow cytometry.

Transfer colitis

To induce transfer colitis, RAG2$^{-/-}$ mice were adoptively transferred with 2 x 10^6 CD4$^+$ CD25$^-$ T cells. Animals were sacrificed as soon as a significant loss of weight was measurable. Spleen and mLNs were harvested for further analysis. One part of the colon was fixed in formalin for histological scoring and the other part was fixed in RNAlater (Qiagen, Germany) for subsequent mRNA analysis. For soluble ST2 (sST2) treatment, mice received 100 µg mouse sST2 (produced by the VIB Protein Core facility and provided by R. Beyaert, VIB-UGent Center for Inflammation Research), three times/week i.p. Control group received PBS i.p. For IL-10R treatment, mice received 500 µg anti IL-10R antibody (1B1mAB) (kindly provided by Prof. Edgar Schmitt, University of Mainz) or IgG control AK (Rat IgG kappa) i.p. once a week during the first three weeks.

Experimental design of ovalbumin-sensitization and ventilation

On day 0, 14 and 21 mice were injected i.p. with ovalbumin (OVA) and aluminium hydroxide (Alu). On day 28, 29 and 34, sensitized mice were exposed to nebulized OVA (1%) for 30 min. Control animals received Alu and were exposed to NaCl (0.9%). On day 35, mice were mechanically ventilated with the flexiVent ventilator (SCIREQ, Canada).

On day of ventilation, mice were tracheotomized with a 20-gauge cannula and connected to a ventilator device with a tidal volume of 10 mL/kg and a positive end-expiratory pressure of 2 cm H_2O. Lung functions were measured by forced oscillation technique (FOT).

Histological scoring

4 µm paraffin sections from the fixed colon were cut serially, mounted onto glass slides, and deparaffinized. The colon sections were stained with hematoxylin and eosin by the Core Facility (IZKF) of the RWTH Aachen University. Blinded histological scoring was performed using a standard microscope, based on TJL method as described previously [38, 39]. Each colon section was scored for the four general criteria: severity, degree of hyperplasia, degree of ulceration, if present, and percentage of area involved. A subjective range of 1-3 (1 = mild, 2 = moderate, 3 = severe) was used for the first three categories. Severity: Focally small or widely separated multifocal areas of inflammation limited to the lamina propria were graded as mild lesions (1). Multifocal or locally extensive areas of inflammation extending to the submucosa were graded as moderate lesions (2). If the inflammation extended to all layers of the intestinal wall or the entire intestinal epithelium was destroyed, lesions were graded as severe (3). Hyperplasia: Mild hyperplasia consisted of morphologically normal lining epithelium that was at least twice as thick (length of crypts) as adjacent or control mucosa. Moderate hyperplasia was characterized by the lining epithelium being two- or three-times normal thickness, cells were hyperchromatic, numbers of goblet cells were decreased, and scattered individual crypts developed an arborizing pattern. Severe hyperplastic regions exhibited markedly thickened epithelium (four or more times normal thickness), marked hyperchromasia of cells, few to no goblet cells, a high mitotic index of cells within the crypts, and numerous crypts with arborizing pattern. Ulceration was graded as: 0 = no ulcer, 1 = 1-2 ulcers (involving up to a total of 20 crypts), 2 = 1-4 ulcers (involving a total of 20-40 crypts), and 3 = any ulcers exceeding the former in size. A 10% scale was used to estimate the area involved in the inflammatory process. 0 = 0%, 1 = 10%-30%, 2 = 40%-70%, 3 = >70%.

Cell isolation

Mouse BM cells were flushed from femurs and tibias with Dulbecco medium. Erythrocytes were lysed with lysis buffer (eBioscience) for 3 min at room temperature, and the remaining cells were washed once with PBS. Single cell suspensions were isolated from spleens and LN using cell strainers and erythrocytes were lysed with lysis buffer. To obtain immune cells from

lung, tissue was excised into small pieces and was digested with 0.1% collagenase in DPBS for 1hr. The digested fraction was passed through a 40µm nylon strainer and rinsed with DPBS. The flow through was centrifuged and the cell pellet was lysed using RBC lysis buffer. The cell pellet was used for the Flow cytometric analysis. Colon was retrieved from the mice and rinsed with a cannula with PBS+0.5%BSA. Afterwards colon was excised into small pieces and placed in a digestive medium containing RPMI (10ml), Collagenase V (0.85mg/ml), Collagenase D (1.25mg/ml), Dispase (1mg/ml) and DNase (30µg/ml) and incubated for 45 minutes at 37°C with gentle shaking. The digested fraction was passed through a 40um nylon strainer and the flow through was collected and centrifuged to obtain a pellet. Percoll gradient centrifugation was performed by using 35% percoll and centrifugation was performed. The cell pellet obtained was lysed using RBC lysis buffer and is used for further analysis. Liver was retrieved from the mice. Gall bladder was removed and liver was excised into small pieces and was placed in a digestive medium containing RPMI without FCS (3ml), 1.25mg/ml Collagenase D and 30µg/ml DNase. The fraction was incubated for 45 minutes and digestion was stopped by adding PBS+0.5% BSA+2mM EDTA and homogenized using a syringe. The digested fraction was passed through a 100µm nylon strainer and the flow through was centrifuged. The pellet obtained was used for the percoll gradient centrifugation by using 35% percoll. The cell pellet obtained after the percoll gradient centrifugation was lysed using RBC lysis buffer and is used for flow cytometric analysis.

Co-Immunoprecipitation (Co-IP)

The Co-IP was carried out to illustrate the complex formation between Foxp3-CREB and Foxp3-CREM. In order to perform this, lymphocytes were isolated from WT mice and purified using nylon columns and were differentiated *in vitro* with 3 µg/ml anti-CD3 und anti-CD28 and 5 ng/ml TGF-β for 5 days. After differentiation, the cells were pelleted and nuclear extracts were isolated and Co-IP was carried out. For the immunoprecipitation of the target protein, the

cell lysate was incubated together with the CREB and CREM antibody. The protein antibody complex was then isolated using an antibody binding protein (protein A or Protein G) coupled to agarose beads. After washing several times, the proteins were separated using SDS-PAGE and were detected by western blot. Input was also included using the 25uL of nuclear extracts.

SDS gel electrophoresis

The proteins were separated according to molecular mass using discontinuous gel electrophoresis. Protein lysates were mixed with SDS sample buffer, transferred to 1.5 ml Eppendorf tubes, heat denatured at 95°C for 5 minutes and sonicated for 2 minutes at 0.5 pulses/min. Lysates were used immediately or stored at −20°C. 25 µl of the samples were filled into the gel pockets. To determine the size, 5 µl of protein markers were also included in one track. The subsequent electrophoresis was carried out at 150 V.

Western blot

The transfer of proteins from SDS gel on to the nitrocellulose paper was carried out using an electrophoretic semi-dry blot apparatus. Blot pads, filter paper and polyacrylamide gel were first soaked in tank buffer; the PVDF membrane was previously activated by placing it in methanol. The protein transfer took place at a mA number, which is the product of the area of the membrane and the factor 1.8, for 70 minutes.

T cell differentiation assays

MACs isolated $CD4^{+}CD25^{-}$ T cells ($2x10^{6}$ per ml) were incubated with plate-coated anti-CD3 (10 µg/ml, eBioscience) and soluble anti-CD28 (eBioscience). $T_{H}0$ cells were left without exogenous cytokines, 5 ng/ml TGF-β was added to induce T_{reg} differentiation.

Flow cytometry

For surface staining, single cell suspensions were stained with anti-CD4, anti-CD3, anti-CD8, anti-CD19, anti-CD25, anti-CD45.1, and anti-CD45.2, anti-GL-7, anti-ICOS, anti-ST2, anti-

Nrp1, anti-PD-1 (all from eBioscience, Germany). For intracellular staining of Foxp3, CTLA-4, Helios, GATA3, T-bet and RORγt, cells were fixed and permeabilized with a FOXP3 staining buffer set (eBioscience, Germany) following the manufacturer's instructions and stained with respective antibodies (eBioscience, Germany) for 30 min. Intracellular cytokines were stained with anti-IFN-γ-Alexa 647 (eBioscience) and anti-IL-17-Alexa 488 (BD), IL-10-APC (ebiosciences), IL-13-FITC antibodies after PMA (30 nM) and Ionomycin (1,5 µM) (both Sigma-Aldrich, USA) restimulation in the presence of Golgi Plug. A daily calibrated FACS-Canto II flow cytometer (Becton Dickinson, MountainView, CA) was used to perform phenotypic analysis. For data analysis FCS-Express 4.0 Research Edition (DeNovo software Glendale, CA, USA) and FlowJo version 10 were used.

Luciferase Assay

RLM cells carrying a stable pGL3-TSDR-FoxPro luciferase plasmid were kindly provided by Jochen Huehn (HZI Braunschweig). Cells were transfected with pcDNA-CREB plasmid or pcDNA. Cells were left to rest over night before luciferase activity was measured by using the Dual-Glo Luciferase Assay System (Promega, USA).

RNA isolation and real-time PCR

Total RNA from isolated T cells and colon tissue was isolated using the RNeasy Mini Kit (Qiagen, Germany). cDNA was then generated from 200 ng total RNA using the RevertAid H Minus First Strand cDNA Synthesis Kit (Thermo Fisher Scientific, USA) according to the manufacturer´s instructions. RT-PCR was performed using the SYBR Green PCR kit (Eurogentec, Germany) and data were acquired with the ABI prism 7300 RT-PCR system (Applied Biosystems / Life Technologies, Germany). Each measurement was set up in duplicate. After normalization to the endogenous reference control gene ß-actin for mice, the relative expression was calculated.

RNA extraction and microarray for gene expression analysis

$CD4^+CD25^+Nrp1^+$ T_{regs} were sorted by FACS. Genome wide transcriptome analyses of $Foxp^{cre}CREB^{fl/fl}$ and WT $CREB^{fl/fl}$) T_{regs} were performed in independent triplicates using Gene Chip® Mouse Gene 2.0 arrays (Affymetrix, Santa Clara, CA, USA). Total RNA extraction was carried out using the RNeasy Micro Kit (Qiagen, Germany) according to manufacturer's protocol and then quantified (Nanodrop). RNA quality was assessed using the RNA 6000 Nano Assay with the 2100 Bioanalyzer (Agilent, Santa Clara, CA, USA). Samples for the Gene 2.0 arrays were prepared and hybridized to the arrays according to the Affymetrix WT Plus Kit manual. Briefly, for each sample, 100 ng of total RNA was reversed transcribed into cDNA using a random hexamer oligonucleotide tagged with a T7 promoter sequence. After second strand synthesis, double strand cDNA was used as a template for amplification with T7 RNA polymerase to obtain antisense cRNA. Random hexamers and dNTPs spiked out with dUTP were then used to reverse transcribe the cRNA into single stranded sense strand cDNA. The cDNA was then fragmented with uracil DNA glycosylase and apurinic/apyrimidic endonuclease 1. Fragment size was checked using the 2100 Bioanalyzer and ranged from 50 to 200 bp. Fragmented sense cDNA was biotin-endlabeled with TdT and probes were hybridized to the Gene 2.0 arrays at 45 °C for 16h with 60 rpms. Hybridised arrays were washed and stained on a Fluidics Station 450 (program: FS450 0002) and scanned on a GeneChip® Scanner 3000 7G (both Affymetrix). Raw image data were analyzed with Affymetrix® Expression Console™ Software (Affymetrix, USA), and gene expression intensities were normalized and summarized with a robust multiarray average algorithm[40]. Transcripts that were expressed differently more than 1.5-fold with a raw p-value lower than 0.05 between the sample groups were categorized as regulated. Enrichment analysis for Wiki pathways was performed using WebGestalt [41]. For the enrichment analysis only genes changed at least 1.5-fold with a p-value lower than 0.05 between $Foxp3^{cre}CREB^{fl/fl}$ and WT ($CREB^{fl/fl}$) samples were taken into consideration.

TSDR Methylation analysis

For all methylation analyses, cells from male mice were used. Genomic DNA was prepared from FACS-sorted Tconv ($CD4^+CD25^-$) as well as Treg cells ($CD4^+CD25^+Nrp1^+$) from $CREB^{fl/fl}$ and $Foxp3^{cre}CREB^{fl/fl}$ mice and subsequently converted by bisulfite according to the manufacturer's instructions (DNeasy Blood & Tissue Kit, Qiagen; EZ DNA Methylation-Lightning Kit, Zymo Research). Pyrosequencing of the Treg cell-specific demethylated region

(TSDR) (chromosome position X:7583950-7584149, genome assembly GRCm38.p6) was performed as described previously [42].

ATAC Sequencing

Omni-ATAC-seq was performed according to [43, 44] with minor modifications. Prior to transposition dead cells were removed by centrifugation (800 rpm, 4 min, 4°C). The transposition reaction was with 7.5 µL Tagment DNA Enzyme 1 (TDE1) for 60 'min at 37°C. Pre-amplification was with NEBNext Ultra II Q5 Master Mix and Nextera PCR Primers (5 cycles). Quantitative PCR amplification was with NEBNext Ultra II Q5 Master Mix, Nextera PCR Primer and SYBR Gold to determine the number of additional cycles. PCR amplification of additional cycles was as for pre-amplification. PCR fragments were purified with Qiagen MinElute PCR Purification Kit and library concentration and quality were determined by Agilent High Sensitive DNA Kit and TapeStation, respectively. ATACseq libraries were sequenced on the Illumina NextSeq 500 Platform with 75 bps paired-end reads in duplicates. ATAC-seq libraries were trimmed with Trim Galore (parameters -q 30 –paired –trim1) and aligned to mouse genome (mm9) using Bowtie2 [45] (parameters -X2000 –no-mixed –no-discordant). Duplicates fragments were removed, and reads were filtered for alignment quality of >Q30 using samtools [46]. Next, we use MAC2 [47] to perform peak calling (parameters –nomodel –nolambda –keep-dup auto –call-summits). Transcription factor footprinting and differential activity was performed using HINT-ATAC as described in [44].

Statistical analysis

All data are presented as mean ± standard error (SEM). Data were tested for normality using Shapiro-Wilk Normality test. Differences between two groups were evaluated using two-tailed unpaired or paired (if indicated), Student's t-test. A two-tailed Mann Whitney test was used, if data were not normally distributed. Measurements were taken from distinct samples. All statistical analysis and subsequent graphics generation were performed using GraphPad Prism version 7.0 and 8.0 (GraphPad Software, USA). A p-value <0.05 was statistically significant.

Study approval

The study was approved by the regional government authorities and animal procedures were performed according to German legislation for animal protection. Permission for the projects was granted by the Regierungspräsident/LANUV Nordrhein-Westfalen.

Data availability

The ATAC-Seq and microarray raw datasets have been deposited in GEO under the accession codes GSE157693 and GSE157933. All data that support the findings of this study are available within the article and Supplementary Files. All other data, including raw data used in each figure will be provided upon reasonable request to the corresponding author.

Results:

VAV^{cre}CREB$^{fl/fl}$ T cells dampen inflammation in experimental colitis

To build upon published findings of Wang et al we performed a transfer of naive CD4+ T cells from *VAVcreCREB$^{fl/fl}$* or appropriate wildtype mice into lymphopenic Rag2$^{-/-}$ mice. In corroboration of the data of Wang transfer of *VAVcreCREB$^{fl/fl}$* CD4+ T cells prevented weight loss (**Fig. 1A**) and recipient mice displayed decreased intestinal inflammation (**Fig. 1B-C**). Furthermore, IFN-γ production in CD4^{+} T cells in the mLN was markedly reduced (**Fig. 1D**), while CD4+ CD25+Foxp3+ expression was enhanced (**Fig. 1E**).

CREB deficiency enhances frequencies of T_{regs} while downregulating their Foxp3 expression

Our data and those of Wang et al. display an enhanced frequency of iTregs in the intestine of transferred mice. To address the question whether this is Treg-intrinsic and not related to CREB deletion in CD4 or VAV, we generated mice with a Foxp3-specific knockout of CREB (*Foxp3^{CRE}CREB$^{fl/fl}$*). It has been described before that CREB stabilizes and promotes Foxp3 expression [11 12, 48, 49]. To our surprise, these mice already showed enhanced numbers of CD25^{+}/Foxp3^{+} positive T_{regs} in the thymus (**Fig. 2A and D**) in addition to spleen (**2B and D**) and peripheral lymph nodes **(Fig. 2C and D**). Expression of Nrp1, PD-1, CTLA4, and ICOS and of the factors GATA3, T-bet and RORγt in Foxp3^{+} cells was not altered (**Supp Fig 1A-F**). However, as expected, *Foxp3^{CRE}CREB$^{fl/fl}$* mice displayed lower Foxp3 expression in T_{regs} on the single cell level (**Fig. 2E and F**) which can be explained by the fact that CREB directly activates the TSDR [11] (**Fig. 2G**). Furthermore, we generated mixed bone marrow chimeric mice. The expression of Foxp3 in *CREB$^{+/+}$*CD45.1 and *CREB$^{-/-}$*CD45.2 T_{reg} cells (CD4^{+}CD25^{+}) was analysed by flow cytometry 8 weeks after bone marrow transfer and was downregulated in *CREB$^{-/-}$*CD45.2 T_{reg} cells (**Fig. 2H and I**). The *CD4^{+}CREB$^{+/+}$*CD45.1 compartment exhibited normal T_{reg} frequencies, whereas percentages of *CREB$^{-/-}$* T_{regs} and expression of Foxp3 in *CREB$^{-/-}$*CD45.2 T_{regs} were markedly reduced (**Fig. 2H)**.

CREB-deficient T_{regs} are suppressive *in vitro*

To test if lower Foxp3 expression affects suppressive capacity of CREB deficient T_{regs}, we co-cultured WT and CREB deficient T_{regs} with anti-CD3 and anti-CD28 stimulated WT $CD4^+$ cells. Interestingly, *Foxp3^{CRE}CREB$^{fl/fl}$* T_{reg} cells revealed an even enhanced capacity to reduce $CD4^+$ T cell proliferation (**Fig. 3A, B**). These data suggest that deletion of CREB, despite reducing Foxp3 expression per cell, does not affect function of T_{regs}. In addition, expression of Helios was enhanced (**Fig. 3C**) and bisulfite sequencing revealed a demethylated TSDR (**Fig. 3D**), which suggests a stable and suppressive phenotype [50] In conclusion, despite reduction of Foxp3 levels per cell, CREB deficiency leads to stable and functional Tregs *in vitro*.

CREB deficient T_{regs} reveal gene expression signature with enhanced expression of IL-10, IL-4, IL-13 and ST2

To understand why CREB deficient T_{regs} are suppressive despite reduced Foxp3 expression, we performed a whole transcriptome analysis (Affymetrix HTA2 arrays) of flow sorted ($CD4^+CD25^+Nrp\text{-}1^+$) *Foxp3^{CRE}CREB$^{fl/fl}$* and *CREB$^{fl/fl}$* T_{regs} (Supp. Fig. 2 A) and appropriate wildtype mice. Using a fold–change of 1.5 and a p-value of less than 0.05 we found 111 downregulated and 122 upregulated genes in the *Foxp3^{cre}Creb$^{fl/fl}$* compared to *CREB$^{fl/fl}$* T_{regs}, among those were IL-10 and IL-13 the 2 most strongly upregulated in the *Foxp3^{cre}Creb$^{fl/fl}$* T_{regs} (**Fig. 4A)**. KEGG pathway analysis revealed an enrichment of differentially regulated genes in pathways that are associated with Th2 cytokines, such as asthma, Th2 and Th2 cell differentiation and cytokine-cytokine receptor interaction pathways (**Fig. 4B**). Higher *Il13 and Il10* mRNA expression in *Foxp3^{cre}Creb$^{fl/fl}$* T_{regs} could be further confirmed by RT-qPCR (**Fig. 4C** and **D**). This partially corroborates the findings of Wang et al. in CD4-CREB-IL17 double knockouts, where they also found a Th2 shift with enhanced IL-4 and IL13 expression in CD4+ T cells, however IL-10 was not affected suggesting a different regulation in Tregs. In our hands, $CD4^+CD25^+Foxp3^+$ cells also showed enhanced IL-10 protein levels after 3 days of CD3/CD28 stimulation as assessed by flow cytometry (Fig. 4 E and F). *In vitro* Treg differentiation with TGF-β revealed a reduced capacity of *Foxp3^{cre}Creb$^{fl/fl}$* T cells to differentiate towards $Foxp3^+$ cells, while IL-10 expressing cells within $Foxp3^+$ cells were expanded. Furthermore IL-10 cytokine expression of Tgf-β stimulated *Foxp3^{cre}Creb$^{fl/fl}$* T cells measured by ELISA was increased as well as *Il13, Il5 and Il10* mRNA expression (**Fig. 4 H-L**). Beyond cytokines, expression of Il1r1 (ST2) showed enhanced expression on the microarray, however splenic CD4 T cells were used for this analysis. ST2, the receptor of IL-33 is preferentially expressed on colonic T_{reg} cells, where it promotes T_{reg} function and adaption to the inflammatory

environment. It provides a necessary signal for T_{reg}-cell accumulation and maintenance in inflamed tissues and it was shown to regulate IL-10 expressing T_{reg} cells in the gut [51]. In addition, IL-33 has been identified as a major interleukin in asthma pathology [52]. ST2 was highly expressed in the *Foxp3^{CRE}CREB$^{fl/fl}$* T_{regs}, which was confirmed by flow cytometry (**Fig. 4 M and N**). Moreover, whole transcriptome analysis also revealed an upregulated expression of CREM in *Foxp3^{cre}CREB$^{fl/fl}$* Treg cells and qRT-PCR also showed tendentially enhanced CREM expression in *Foxp3^{cre}CREB$^{fl/fl}$* Treg cells **(Fig. 4O**). In conclusion, these data suggest that CREB deletion induces a ST2 positive Th2 biased phenotype in T_{regs}.

Genome-wide chromatin accessibility of WT and CREB-deficient T_{regs} reveals differences in the IL13, ST2 and CREM region.

To analyse if CREB deletion alters chromatin accessibility, we performed the Assay for Transposase-Accessible Chromatin using sequencing (ATAC-seq) in splenic CD4+CD25+Nrp+ T cells. We observe a decrease in open chromatin around CREB1 and CREM (CRE) motifs on *Foxp3^{Cre}CREB$^{fl/fl}$* mice, which indicate loss of binding activity of these TFs in these cells (**Fig. 5 A**). The *l1rl1* (ST2) region showed small but significant differences in open chromatin around the promoter as well as potential enhancer sites in T_{reg} cells of *Foxp3^{Cre}CREB$^{fl/fl}$* mice, while CREB-binding motifs could not be detected (**Fig. 5 B**). These differences were identified in the original promoter as well as in an alternative promoter region, which has been very recently identified as being important for type 1 antiviral T-cell responses. This promoter is selectively activated in CD8 T cells during antiviral immune responses has not been described in Tregs before. This finding together with the increased mRNA expression of ST2 led us investigate the protein expression of ST2 within different organs in ***Foxp3^{cre}CREB$^{fl/fl}$ROSA^{RFP}*** mice. As shown in **Figure 5 F-J**, ST2 expression was clearly enhanced in T_{regs} in the thymus, spleen, mesenteric lymph nodes, lung and colon of these mice.

Moreover, the IL-13 enhancer region showed differences between the two mice strains. Within this region, binding sites for Nrf1 were identified, which is a CREB related transcription factor. As expected, we found a change in open chromatin of an alternate promoter of CREM (**Fig. 5 B**). CREM has been identified as one of the most regulated genes in ST2 positive colonic Tregs of healthy mice [53]. To proof if CREM is involved in the regulation of ST2 we generated *Foxp3^{cre}CREB$^{fl/fl}$-CREM$^{-/-}$* mice. *In vitro* differentiation towards Foxp3^{+} cells was not significantly diminished in *Foxp3^{cre}CREB$^{fl/fl}$-CREM$^{-/-}$* mice (**Fig. 5C**). Furthermore, deletion of CREM normalized Foxp3 expression per cell in CREB-deficient Tr_{egs} at least to some extent (**Fig. 5D**), however completely reversed expression of ST2 (**Fig 5E**). Taken together our data

suggest that the interaction of CREB and CREM are of relevance for the expression of ST2 and induction of CREM in CREB deficient T_{regs} contributes to reduced Foxp3 expression.

CREM and CREB both interact with Foxp3

The open chromatin structure of both ST2 promoters in Tregs does not contain any CRE site and the chromatin structure of the IL-10 promoter measured by ATACseq is not altered while expression is strikingly different and specific to Tregs, as Wang et al did not demonstrate this in CD4 T cells. It was published before that ST2 positive Tregs are Th2 biased and produce more IL-10, however the mechanism has not been elucidated yet. IL-10 expression undergoes cell type specific regulations at different levels (including open chromatin) and is definitively dependent on Foxp3 expression, while no binding sites of Foxp3 have been found in the promoter and enhancer regions. As an alternate mechanism, it has been recently described that Foxp3 affects transcription by bridging of DNA in a three-dimensional context using different interaction partners. We therefore asked, whether CREM and CREB would be suitable intracellular partners of Foxp3. As shown in figure **6 A and B**, both CREM and CREB can be detected by CO-IP analysis as cooperating partners of Foxp3. This finding could be of significance for transcriptional alterations and thus functional capacities of Tregs.

Transfer of *Foxp3^{cre}CREB$^{fl/fl}$* CD4+CD25- T cells prevents experimental colitis

Our previous data showed enhanced T_{reg} frequencies already in the thymus as well as in the spleen and different peripheral organs of *Foxp3creCREB$^{fl/fl}$* mice. To test, whether iTreg expansion is also enhanced during inflammation in the ***Foxp3^{cre}CREB$^{fl/fl}$*** T cells, we transferred CD4+CD25- T cells of *Foxp3creCREB$^{fl/fl}$* T cells or appropriate wildtype T cells into lymphopenic Rag2$^{-/-}$ mice (without co-transfer of T_{regs}). Strikingly, transfer of *Foxp3^{cre}CREB$^{fl/fl}$* CD4+ T cells again again prevented weight loss (**Fig. 7A**) and recipient mice displayed decreased intestinal inflammation (**Fig. 7B** and **C**). Furthermore, inflammatory cytokines in the gut were markedly reduced (**Fig. 7D**) as well as IL-17 and IFN-γ production in CD4^{+} T cells in the mLN (**Fig. 7E-G**). The experiment was repeated with CD4+RFP- T cells of *Foxp3^{cre}CREB$^{fl/fl}$ ROSA^{RFP}* mice into Rag2-/- mice, which allows for the tracing of these cells upon iTreg induction and showed the same results. The transfer of CD4+RFP- T cells of

Foxp3^{cre}*CREB*$^{fl/fl}$ *ROSA*^{RFP} mice prevented development of colitis and resulted in enhanced accumulation of RFP+ T_{regs} also in different organs (**Fig. 8A-G**) without signs of inflammation. The findings of these 2 transfer experiments with two independent genetic strains are thus in contrast to the mixed bonemarrow chimera results and suggest clear intrinsic mechanisms that drive expansion of these cells in different peripheral organs.

Blockade of IL-10 reverses protective effects of *Foxp3*^{cre}*CREB*$^{f/f}$ T cells in experimental colitis

We have shown before that the CREB deficient Tregs cells are protective in intestinal inflammation and release IL-10 [54]. To decipher if *Foxp3*^{cre}*CREB*$^{fl/fl}$ T cells prevent colitis by IL-10 production and/or ST2 expression, we performed an adoptive transfer colitis with anti-IL10R antibodies or recombinant soluble ST2 (sST2). sST2 acts as a decoy for IL-33 and inhibits its biological activity [55]. Blockade of IL-10 signalling induced a colitis in the former resistant *Foxp3*^{cre}*CREB*$^{fl/fl}$ T cell recipient mice (**Fig. 9A-C**), while ST2 blockade had no effect on disease progression (**Supp. Fig. 3A**). We had nevertheless shown before in figure 5, that additional genetic deletion of CREM reverses ST2 expression which is in line with finding of the group of Fiona Powrie that CREM is upregulated in ST2 positive Tregs in the gut. We therefore performed the transfer colitis with naïve CD4+ T cells from *Foxp3*^{cre}*CREB*$^{fl/fl}$ *CREM-/-* mice. As depicted in **Figure 9 D-H**, the additional genetic deletion of CREM resulted in histological reversal of the colitis phenotype. Rag2-/- mice transferred with CD4+ cells of *Foxp3*^{cre}*CREB*$^{fl/fl}$ *CREM-/-* mice kept their weight **(Fig. 9D)** compared to their wild type littermates however displayed a more severe histological phenotype (**Fig. 9E**). Decreased frequencies of CD4+ T cell percentages were found in Rag2-/- mice transferred with CD4+ cells of *Foxp3*^{cre}*CREB*$^{fl/fl}$ *CREM-/-* mice **(Fig. 9F).** No differences were observed in the frequencies of IFN-γ and IL-10 expression (**Fig. 9 G-H**).

Foxp3^{CRE}*CREB*$^{fl/fl}$ mice display enhanced asthma phenotype

It was shown before, that reduction of Foxp3 in T_{regs} induces a dominant type 2 immunity in mice [56, 57]. Moreover, it was demonstrated that ST2 positive Tregs promote asthmatic responses (IL33 asthma Paper). Despite the fact that our mice are bred on a non-atopic C57/Bl background, we could observe spontaneous development of higher level of IgEs but not IgGs in sera of aged mice (**Fig. 10A**). These results suggest enhanced spontaneous type 2 immune

responses in these mice. To further analyse this *in vivo,* we performed an OVA-induced asthma model, for which again, another background like Balb/c would have been more suitable. Mice were sensitized with OVA and subsequently lung function measurements were performed 35 days after OVA challenges. *Foxp3^{Cre}CREB$^{fl/fl}$* mice clearly displayed worsened lung function parameters upon OVA- challenge including enhanced resistance Rrs and elastance Ers and also worsened function of the smaller airways (exemplarily tissue damping H, **Fig. 10 B-D**) compared to their wild type littermates. In addition, we observed enhanced percentages of ST2^{+} T_{regs} within the BAL of *Foxp3^{Cre}CREB$^{fl/fl}$* mice (**Fig. 10 E-F**). As described before, OVA-sensitization increases ST2 expression on T_{regs} also in wild type mice (from 2.5 to 10%), while in *Foxp3^{Cre}CREB$^{fl/fl}$* mice average expression was around 30%. In contrast we found very little expression of Th2 cytokines in the BAL between the *Foxp3^{Cre}CREB$^{fl/fl}$* and wildytpe mice and thus no differences could be detected. Our explanation for this fact is again the genetic background of the mice, which prevents the expression of high levels of type 2 cytokines.

Discussion:

In this study we provide evidence that CREB unexpectedly is dispensible for tTreg and iTreg expression and function. Instead, genetic deletion of CREB enhanced numbers of ST2 positive Tregs in different lymphoid and nonlymphoid organs including the thymus combined with enhanced IL-10 expression, which resulted in the prevention of T cell mediated colitis. This however comes at the costs of enhanced type 2 immune responses and asthma severity. In addition, we can show that the ST2 transcription is dependent on CREB and CREM expression, since additional genetic deletion of CREM prevented the upregulation of ST2 and prevented the protective effect in the transfer colitis model. Mechanistically, there is a moderate alteration in chromatin accessibility at both ST2 promoters and no difference in chromatin accessibility at the IL-10 promoter. However, we show that both, CREB and CREM, are able to interact with Foxp3 and it is possible that this interaction might alter transcription of e.g. IL-10 in Tregs. This seems to be specific for Tregs, since it has not been described in CD4 T cells in the publication of Wang et al. There have no Foxp3 bindings sites identified on the IL-10 promoter and enhancer so far, nevertheless, Tregs are characterized by a Foxp3 dependent expression of IL-10 and IL10 mediated repression is one of the functional hallmarks of Tregs.

We have shown that the enhanced IL-10 secretion prevented colitis in Rag-/- mice transferred with *Foxp3^{cre}CREB$^{fl/fl}$* CD4+ T cells. IL-10 is an important regulator of intestinal homeostasis, as IL10 and IL10R deficient mice spontaneously develop intestinal inflammation [63, 64] and blocking IL-10 signalling induced colitis in *Foxp3^{cre}CREB$^{fl/fl}$* T cell recipients that were

previously resistant. It was demonstrated before that CREB induces IL-10 transcription in macrophages. Our data thus were unexpected and do not support these findings but might instead again argue for Treg-specific mechanisms including interaction of CREB and CREM with Foxp3 that regulate IL-10 expression. In line with this, *Foxp3^{cre}CREB$^{fl/fl}$* T_{reg} displayed enhanced levels of the IL-33R ST2. ST2, the receptor of IL-33 is preferentially expressed on colonic T_{reg} cells, where it promotes T_{reg} function and adaption to the inflammatory environment. It provides a necessary signal for T_{reg}-cell accumulation and maintenance in inflamed tissues and it was shown to regulate IL-10 expressing T_{reg} cells in the gut [51]. Interestingly, CREM expression, which was enhanced in *Foxp3^{cre}CREB$^{fl/fl}$* T_{reg} was found before as a highly regulated gene in ST2 positive colon and skin T_{regs} [53]. We additionally found higher ST2 expression on Tregs in different other organs including the lung resulting in the asthma phenotype. It was previously published that Tregs, which are cultured in the presence of IL33, display high *Il5* and *Il13* mRNA however no differences in the levels of Gata3 and Foxp3 mRNA. This strikingly corroborates our transcriptional findings in the *Foxp3^{cre}CREB$^{fl/fl}$* Tregs. In parallel, $ST2^+$ Treg cells from mice exposed to allergens also show a significant increase in *Il5* and *Il13* mRNA expression compared with those from PBS-exposed mice. These findings suggest that, similar to the results in IL-33–exposed mice numbers of T_H2 cell–like Treg cells increase in the lungs during allergen-induced airway inflammation and that self-perpetuating effects of IL-33 on lung Treg cells exist.

We were able to demonstrate that iTRegs generated from naïve CD4 positive cells from *Foxp3^{cre}CREB$^{fl/fl}$* mice also display the heightened expression of ST2 in different organs including the lung, which could be related to enhanced migratory potential.

The migratory potential of ST2 has not been described in T cells and Tregs, however in other cell types. In patients with alcoholic hepatitis, a defect in the IL-33/ST2 pathway in neutrophils is associated with lower migration capacities and a higher probability of getting infected. Administration of IL-33 to the neutrophils at least partly restores this defect. Furthermore, in several tumor models, IL-33 promotes the migration and metastasis of the tumor cells. Finally and more importantly, IL-33 modulates migration of hematopoietic progenitor cells in patients with allergic asthma, suggesting that enhanced expression of ST2 could also enhance migratory potential of these cells.

Delacher et al. characterized ST2-positive tissue T_{regs} that are present in all nonlymphoid tissues, which were found to express killer cell lectin-like receptor subfamily G1 (KLRG1) and Th2 associated factors, including IL-10 [15, 65]. These “tisTregsST2” cells are programmed by

Basic leucine zipper transcription factor ATF-like (BATF) [65] in lymphoid organs, and perform important tissue homeostasis and regenerative functions. We now show that CREB also regulates tisTregsST2 in non-lymphoid tissues.

In conclusion, we provide evidence that CREB plays a pivotal role in T_{regs}. CREB is an important transcription factor to maintain Foxp3 expression and prevent exaggerated type 2 responses. On the other hand, lack of CREB enhances IL-10 expression and thereby prevents Th1 mediated diseases. Our study has been focused on mouse T_{regs}. Further studies will show how CREB affects human T_{regs} and how this translates to human type 2 -mediated diseases including allergy and asthma and whether targeting of CREB could on the other hand be useful in diseases that benefit from high IL-10 expression, such as inflammatory bowel disease.

Acknowledgment:

This research project was supported by DFG grant TE339/20-1. The authors acknowledge the IZKF Flow Cytometry Facility and Genomics Facility for their service.

Author Contributions:

SHS & KO conducted the experiments, analyzed data and wrote the manuscript, JH, SS, TL, TG, CN, TC, MS, EV, SB, & SF conducted experiments, MK contributed to study design, IC, ZL, LG, BD, & SF analyzed data, JH & MZ analyzed data and contributed to study design, ES, RB, & BL provided reagents, TB provided mice and contributed to study design, NW contributed to writing the manuscript, KO & KT designed the study.

References:

1. Wildin, R.S. *et al.* X-linked neonatal diabetes mellitus, enteropathy and endocrinopathy syndrome is the human equivalent of mouse scurfy. *Nat Genet* **27**, 18-20 (2001).

2. Bennett, C.L. *et al.* The immune dysregulation, polyendocrinopathy, enteropathy, X-linked syndrome (IPEX) is caused by mutations of FOXP3. *Nat Genet* **27**, 20-21 (2001).

3. Zhou, X. *et al.* Instability of the transcription factor Foxp3 leads to the generation of pathogenic memory T cells in vivo. *Nat Immunol* **10**, 1000-1007 (2009).

4. Setoguchi, R., Hori, S., Takahashi, T. & Sakaguchi, S. Homeostatic maintenance of natural Foxp3(+) CD25(+) CD4(+) regulatory T cells by interleukin (IL)-2 and induction of autoimmune disease by IL-2 neutralization. *J Exp Med* **201**, 723-735 (2005).

5. Liao, W., Lin, J.X. & Leonard, W.J. IL-2 family cytokines: new insights into the complex roles of IL-2 as a broad regulator of T helper cell differentiation. *Curr Opin Immunol* **23**, 598-604 (2011).

6. Zorn, E. *et al.* IL-2 regulates FOXP3 expression in human CD4+CD25+ regulatory T cells through a STAT-dependent mechanism and induces the expansion of these cells in vivo. *Blood* **108**, 1571-1579 (2006).

7. Ohl, K. & Tenbrock, K. Regulatory T cells in systemic lupus erythematosus. *Eur J Immunol* **45**, 344-355 (2015).

8. Lal, G. & Bromberg, J.S. Epigenetic mechanisms of regulation of Foxp3 expression. *Blood* **114**, 3727-3735 (2009).

9. Baron, U. *et al.* DNA demethylation in the human FOXP3 locus discriminates regulatory T cells from activated FOXP3(+) conventional T cells. *Eur J Immunol* **37**, 2378-2389 (2007).

10. Floess, S. *et al.* Epigenetic control of the foxp3 locus in regulatory T cells. *PLoS Biol* **5**, e38 (2007).

11. Kim, H.P. & Leonard, W.J. CREB/ATF-dependent T cell receptor-induced FoxP3 gene expression: a role for DNA methylation. *J Exp Med* **204**, 1543-1551 (2007).

12. Polansky, J.K. *et al.* Methylation matters: binding of Ets-1 to the demethylated Foxp3 gene contributes to the stabilization of Foxp3 expression in regulatory T cells. *J Mol Med (Berl)* **88**, 1029-1040 (2010).

13. Tsuji, M. *et al.* Preferential generation of follicular B helper T cells from Foxp3+ T cells in gut Peyer's patches. *Science* **323**, 1488-1492 (2009).

14. Wang, Y., Souabni, A., Flavell, R.A. & Wan, Y.Y. An intrinsic mechanism predisposes Foxp3-expressing regulatory T cells to Th2 conversion in vivo. *J Immunol* **185**, 5983-5992 (2010).

15. Delacher, M. *et al.* Genome-wide DNA-methylation landscape defines specialization of regulatory T cells in tissues. *Nat Immunol* **18**, 1160-1172 (2017).

16. Bodor, J. *et al.* Cyclic AMP underpins suppression by regulatory T cells. *Eur J Immunol* **42**, 1375-1384 (2012).

17. Bopp, T. *et al.* Cyclic adenosine monophosphate is a key component of regulatory T cell-mediated suppression. *J Exp Med* **204**, 1303-1310 (2007).

18. Okamoto, A., Fujio, K., Okamura, T. & Yamamoto, K. Regulatory T-cell-associated cytokines in systemic lupus erythematosus. *J Biomed Biotechnol* **2011**, 463412 (2011).

19. Rubtsov, Y.P. *et al.* Regulatory T cell-derived interleukin-10 limits inflammation at environmental interfaces. *Immunity* **28**, 546-558 (2008).

20. Murai, M. *et al.* Interleukin 10 acts on regulatory T cells to maintain expression of the transcription factor Foxp3 and suppressive function in mice with colitis. *Nat Immunol* **10**, 1178-1184 (2009).

637
638 21. Unutmaz, D. & Pulendran, B. The gut feeling of Treg cells: IL-10 is the silver lining during
639 colitis. *Nat Immunol* **10**, 1141-1143 (2009).

640
641 22. Brenner, S. *et al.* cAMP-induced Interleukin-10 promoter activation depends on
642 CCAAT/enhancer-binding protein expression and monocytic differentiation. *J Biol Chem* **278**,
643 5597-5604 (2003).

644
645 23. Sanin, D.E., Prendergast, C.T. & Mountford, A.P. IL-10 Production in Macrophages Is
646 Regulated by a TLR-Driven CREB-Mediated Mechanism That Is Linked to Genes Involved in
647 Cell Metabolism. *J Immunol* **195**, 1218-1232 (2015).

648
649 24. De Cesare, D. & Sassone-Corsi, P. Transcriptional regulation by cyclic AMP-responsive factors.
650 *Progress in nucleic acid research and molecular biology* **64**, 343-369 (2000).

651
652 25. Sassone-Corsi, P. Transcription factors responsive to cAMP. *Annu Rev Cell Dev Biol* **11**, 355-
653 377 (1995).

654
655 26. Foulkes, N.S., Borrelli, E. & Sassone-Corsi, P. CREM gene: use of alternative DNA-binding
656 domains generates multiple antagonists of cAMP-induced transcription. *Cell* **64**, 739-749
657 (1991).

658
659 27. Barton, K. *et al.* Defective thymocyte proliferation and IL-2 production in transgenic mice
660 expressing a dominant-negative form of CREB. *Nature* **379**, 81-85 (1996).

661
662 28. Powell, J.D., Lerner, C.G., Ewoldt, G.R. & Schwartz, R.H. The -180 site of the IL-2 promoter is
663 the target of CREB/CREM binding in T cell anergy. *J Immunol* **163**, 6631-6639 (1999).

664
665 29. Ohl, K., Wiener, A., Schippers, A., Wagner, N. & Tenbrock, K. IL-2 treatment reverses effects
666 of CREMalpha-overexpressing T cells in autoimmune-prone mice. *Clinical and experimental*
667 *immunology* (2015).

668
669 30. Lippe, R. *et al.* CREMalpha overexpression decreases IL-2 production, induces a T(H)17
670 phenotype and accelerates autoimmunity. *J Mol Cell Biol* **4**, 121-123 (2012).

671
672 31. Via, C.S., Tsokos, G.C., Bermas, B., Clerici, M. & Shearer, G.M. T cell-antigen-presenting cell
673 interactions in human systemic lupus erythematosus. Evidence for heterogeneous expression
674 of multiple defects. *J Immunol* **151**, 3914-3922 (1993).

675
676 32. Solomou, E.E., Juang, Y.T., Gourley, M.F., Kammer, G.M. & Tsokos, G.C. Molecular basis of
677 deficient IL-2 production in T cells from patients with systemic lupus erythematosus. *J*
678 *Immunol* **166**, 4216-4222 (2001).

679

33. Asahara, H. *et al.* Chromatin-dependent cooperativity between constitutive and inducible activation domains in CREB. *Mol Cell Biol* **21**, 7892-7900 (2001).

34. Tenbrock, K., Juang, Y.T., Leukert, N., Roth, J. & Tsokos, G.C. The transcriptional repressor cAMP response element modulator alpha interacts with histone deacetylase 1 to repress promoter activity. *J Immunol* **177**, 6159-6164 (2006).

35. Hedrich, C.M., Rauen, T. & Tsokos, G.C. cAMP-responsive element modulator (CREM)alpha protein signaling mediates epigenetic remodeling of the human interleukin-2 gene: implications in systemic lupus erythematosus. *J Biol Chem* **286**, 43429-43436 (2011).

36. Okawa, H. *et al.* Hepatocyte-specific deletion of the keap1 gene activates Nrf2 and confers potent resistance against acute drug toxicity. *Biochem Biophys Res Commun* **339**, 79-88 (2006).

37. Ruther, B.J. *et al.* Combination of cuprizone and experimental autoimmune encephalomyelitis to study inflammatory brain lesion formation and progression. *Glia* **65**, 1900-1913 (2017).

38. Bleich, A. *et al.* Refined histopathologic scoring system improves power to detect colitis QTL in mice. *Mamm Genome* **15**, 865-871 (2004).

39. Pils, M.C. *et al.* Commensal gut flora reduces susceptibility to experimentally induced colitis via T-cell-derived interleukin-10. *Inflamm Bowel Dis* **17**, 2038-2046 (2011).

40. Irizarry, R.A. *et al.* Exploration, normalization, and summaries of high density oligonucleotide array probe level data. *Biostatistics* **4**, 249-264 (2003).

41. Wang, J., Duncan, D., Shi, Z. & Zhang, B. WEB-based GEne SeT AnaLysis Toolkit (WebGestalt): update 2013. *Nucleic Acids Res* **41**, W77-83 (2013).

42. Garg, G. *et al.* Blimp1 Prevents Methylation of Foxp3 and Loss of Regulatory T Cell Identity at Sites of Inflammation. *Cell Rep* **26**, 1854-1868 e1855 (2019).

43. Corces, M.R. *et al.* An improved ATAC-seq protocol reduces background and enables interrogation of frozen tissues. *Nat Methods* **14**, 959-962 (2017).

44. Li, Z. *et al.* Identification of transcription factor binding sites using ATAC-seq. *Genome Biol* **20**, 45 (2019).

45. Langmead, B. & Salzberg, S.L. Fast gapped-read alignment with Bowtie 2. *Nat Methods* **9**, 357-359 (2012).

723 46. Li, H. *et al.* The Sequence Alignment/Map format and SAMtools. *Bioinformatics* **25**, 2078-
724 2079 (2009).

725
726 47. Zhang, Y. *et al.* Model-based analysis of ChIP-Seq (MACS). *Genome Biol* **9**, R137 (2008).

727
728 48. Ruan, Q. *et al.* Development of Foxp3(+) regulatory t cells is driven by the c-Rel
729 enhanceosome. *Immunity* **31**, 932-940 (2009).

730
731 49. Zheng, Y. *et al.* Role of conserved non-coding DNA elements in the Foxp3 gene in regulatory
732 T-cell fate. *Nature* **463**, 808-812 (2010).

733
734 50. Thornton, A.M. *et al.* Helios(+) and Helios(-) Treg subpopulations are phenotypically and
735 functionally distinct and express dissimilar TCR repertoires. *Eur J Immunol* **49**, 398-412
736 (2019).

737
738 51. Schiering, C. *et al.* The alarmin IL-33 promotes regulatory T-cell function in the intestine.
739 *Nature* **513**, 564-568 (2014).

740
741 52. Drake, L.Y. & Kita, H. IL-33: biological properties, functions, and roles in airway disease.
742 *Immunol Rev* **278**, 173-184 (2017).

743
744 53. Miragaia, R.J. *et al.* Single-Cell Transcriptomics of Regulatory T Cells Reveals Trajectories of
745 Tissue Adaptation. *Immunity* **50**, 493-504 e497 (2019).

746
747 54. Siede, J. *et al.* IL-33 Receptor-Expressing Regulatory T Cells Are Highly Activated, Th2 Biased
748 and Suppress CD4 T Cell Proliferation through IL-10 and TGFbeta Release. *PLoS One* **11**,
749 e0161507 (2016).

750
751 55. Holgado, A. *et al.* IL-33trap is a novel IL-33-neutralizing biologic that inhibits allergic airway
752 inflammation. *J Allergy Clin Immunol* **144**, 204-215 (2019).

753
754 56. Juang, Y.T. *et al.* Systemic lupus erythematosus serum IgG increases CREM binding to the IL-2
755 promoter and suppresses IL-2 production through CaMKIV. *J Clin Invest* **115**, 996-1005
756 (2005).

757
758 57. Sawant, D.V. *et al.* Bcl6 controls the Th2 inflammatory activity of regulatory T cells by
759 repressing Gata3 function. *J Immunol* **189**, 4759-4769 (2012).

760
761 58. Hansmann, L. *et al.* Dominant Th2 differentiation of human regulatory T cells upon loss of
762 FOXP3 expression. *J Immunol* **188**, 1275-1282 (2012).

763
764 59. Wan, Y.Y. & Flavell, R.A. Regulatory T-cell functions are subverted and converted owing to
765 attenuated Foxp3 expression. *Nature* **445**, 766-770 (2007).

60. Van Gool, F. *et al.* A Mutation in the Transcription Factor Foxp3 Drives T Helper 2 Effector Function in Regulatory T Cells. *Immunity* **50**, 362-377 e366 (2019).

61. Pelly, V.S. *et al.* Interleukin 4 promotes the development of ex-Foxp3 Th2 cells during immunity to intestinal helminths. *J Exp Med* **214**, 1809-1826 (2017).

62. Wang, X. *et al.* Cyclic AMP-Responsive Element-Binding Protein (CREB) is Critical in Autoimmunity by Promoting Th17 but Inhibiting Treg Cell Differentiation. *EBioMedicine* **25**, 165-174 (2017).

63. Kuhn, R., Lohler, J., Rennick, D., Rajewsky, K. & Muller, W. Interleukin-10-deficient mice develop chronic enterocolitis. *Cell* **75**, 263-274 (1993).

64. Spencer, S.D. *et al.* The orphan receptor CRF2-4 is an essential subunit of the interleukin 10 receptor. *J Exp Med* **187**, 571-578 (1998).

65. Delacher, M. *et al.* Precursors for Nonlymphoid-Tissue Treg Cells Reside in Secondary Lymphoid Organs and Are Programmed by the Transcription Factor BATF. *Immunity* **52**, 295-312 e211 (2020).

Figure 1: *Vav^{cre}Creb$^{fl/fl}$* CD4+ T cells induce only moderate inflammation in experimental colitis. Rag$^{-/-}$ mice were adoptively transferred with CD4^{+} wild-type cells (*CREB$^{fl/fl}$* CD4^{+}) or *Vav^{CRE}CREB$^{fl/fl}$* CD4^{+} T cells. Untreated Rag$^{-/-}$ mice were used as controls (K). Mice were weighed and sacrificed 5 weeks after transfer. (A) Body weight as a percent of starting weight. (B) Representative photomicrographs of hematoxylin and eosin (H&E)-stained colon sections imaged using a 10 x objective. C) Results of histological TJL (The Jackson Laboratory Score) scoring of colon sections (one independently performed experiments, *CREB$^{fl/fl}$* recipients N = 3, *VAV^{cre}CREB$^{fl/fl}$* recipients N = 4). D) Statistical analysis of IFNy within CD4^{+} cells in spleen and mLNs (*CREB$^{fl/fl}$* recipients N = 3, *VAV3^{cre}CREB$^{fl/fl}$* recipients N = 4), a two-tailed, unpaired t-test was used. E) Statistical analysis of CD25+Foxp3+ within CD4^{+} cells in spleen and mLNs (*CREB$^{fl/fl}$* recipients N = 3, *VAV3^{cre}CREB$^{fl/fl}$* recipients N = 4), a two-tailed, unpaired t-test was used.

Figure 2: Genetic deletion of CREB in Foxp3^{+} cells downregulate Foxp3 expression in T$_{regs}$.
A) Statistical analysis of splenic T$_{reg}$ (CD4^{+}CD25^{+}Foxp3^{+}) percentages from *CREB$^{fl/fl}$* and *Foxp3^{cre}CREB$^{fl/fl}$* mice (*N* = 9, 4 independently performed experiments, each with 2-3 age and sex-

matched mice, 6-9 weeks old). **B)** Statistical analysis of T_{reg} percentages within thymus ($CD3^+CD4^{sp}CD25^+Foxp3^+$) from *CREB*$^{fl/fl}$ and *Foxp3*^{cre}*CREB*$^{fl/fl}$mice (*N* = 7, 3 independently performed experiments, each with 2-3 age and sex-matched mice, 6-9 weeks old). **C)** Statistical analysis of T_{reg} ($CD4^+CD25^+Foxp3^+$) percentages from pLN from *CREB*$^{fl/fl}$ and *Foxp3*^{cre}*CREB*$^{fl/fl}$ (*N* =5, 2 independently performed experiments, each with 2-3 age and sex-matched mice 7-9 weeks old). **D)** Density plot showing $CD25^+Foxp3^+$ cells gated on $CD3^+CD4^+CD8^-$ cells in thymus of *CREB*$^{fl/fl}$ and *Foxp3*^{cre}*CREB*$^{fl/fl}$ mice (left), $CD25^+Foxp3^+$ cells gated on $CD4^+$ cells in spleens of *CREB*$^{fl/fl}$ and *Foxp3*^{cre}*CREB*$^{fl/fl}$ mice (middle) and $CD4^+CD25^+$Foxp3+ cells in pLN of *CREB*$^{fl/fl}$ and *Foxp3*^{cre}*CREB*$^{fl/fl}$ mice (right). **E**) Statistical analysis of mean fluorescent intensity (MFI) of Foxp3 in *CREB*$^{fl/fl}$ and *Foxp3*^{cre}*CREB*$^{fl/fl}$ $CD4^+CD25^+$ T cells (*N=6*, 3 independently performed experiments, each with 2 animals, 6-8 weeks old,sex and age matched). **F**) Representative histogram showing overlay of Foxp3 expression in $CD4^+CD25^+$ cells from *CREB*$^{fl/fl}$(black) and *Foxp3*^{cre}*CREB*$^{fl/fl}$ (grey) spleens. **G)** RLM cells carrying a stable pGL3-TSDR-FoxPro luciferase Plasmid were transfected either with an empty vector or CREB plasmid, stimulated with PMA and luciferase activity was measured after 4 hours (*N = 5*). **H)** BM chimeric mice were analyzed 8 weeks after transfer of a mix of CD45.1 WT and CD45.2 *Foxp3*^{cre}*CREB*$^{fl/fl}$ BM cells into lethally irradiated *RAG2*$^{-/-}$ recipient mice (*N = 3*). Percentages of splenic $CD4^+CD25^+Foxp3^+$ T cells of CD45.1 and CD45.2 origin in mixed bone marrow chimeras and bone marrow chimeras. **I)** Statistical analysis of Foxp3 MFI in splenic $CD4^+CD25^+$ T cells within $CD45.2^+$ and $CD45.1^+$ cell populations of 3 mixed bone-marrow chimeras. For A, B, C, E, H, I two-tailed, unpaired t-tests were used to test significance. For G a one-sample test was used. All results are expressed as the mean ± SEM.

Figure 3: *In vitro* suppressive capacity of T_{regs} is enhanced in the absence of CREB. A) WT $CD4^+$ T cells (T_{eff}) from spleens were labeled with efluor660 and stimulated with anti-CD3/CD28 antibodies. $CD4^+CD25^+$ T cells (T_{regs}) from *CREB*$^{fl/fl}$ or *Foxp3*^{cre}*CREB*$^{fl/fl}$ animals were added in different ratios. The proliferation of responder T cells was assessed by efluor (ebioscience) dilution (*N = 3*) B) Representative density plots of A). C) Statistical analysis of MFI of Helios in *CREB*$^{fl/fl}$ and Foxp3^{cre}*CREB*$^{fl/fl}$ $CD4^+Foxp3^+$ T cells (*N = 5*, 2 independently performed experiments, each with 2-3 animals, 8 weeks old sex-matched). D) Representative TSDR methylation patterns of purified $CD4^+CD25^+Nrp1^+$ Treg cells and $CD4^+CD25^-$ conventional T cells from spleens of isolated from 6-8

weeks old male mice (*N = 4*). Amplicons are vertically arranged, each representing a single CpG-motif. The methylation rate of each motif was translated into a yellow-green-blue color code.

Fig. 4: Altered gene expression in CREB deficient T_{regs}. A) Gene expression in T_{regs} from spleens of $CREB^{fl/fl}$ and *$Foxp3^{cre}CREB^{fl/fl}$ mice.* Colors indicate significant upregulation or downregulation of at least 1,5-fold with p-value not more than 0.05 (blue); regulation of at least 1,5-fold or regulation with p-value not more than 0.05 (red). B) Selection of pathways and associated genes, which were significantly enriched. C) N-fold *Il13* mRNA expression in splenic T_{regs} from from *$CREB^{fl/fl}$* and *$Foxp3^{cre}CREB^{fl/fl}$* mice (*N = 5*, male, 8-10 weeks old) analyzed by RT-qPCR. Bars indicate mean and error bars SEM, two-tailed one-sample test. D) N-fold *Il10* mRNA expression in splenic T_{regs} from from *$CREB^{fl/fl}$* and *$Foxp3^{cre}CREB^{fl/fl}$* mice (*N = 5*, male, 8-10 weeks old) analyzed by RT-qPCR. Bars indicate mean and error bars SEM, two-tailed one sample test. E) MACS-isolated T cells from spleens were stimulated *ex-vivo* with anti-CD3/CD28 antibodies for three days and re-stimulated with PMA/Ionomycin in the presence of Golgi Plug™. A representative density plot shows IL-10 production in $CD4^+Foxp3^+$ cells F) Statistical analysis of IL-10 expression of $Foxp3^+$ cells after treatment as in E) (*N = 3* independent experiments, each dot represents one animal, two tailed unpaired t-test. G) $CD4^+CD25^-$ T cells were stimulated with anti-CD3/CD28 antibodies in the presence/absence of 5 ng/ml TGF-β for five days. Percentages of $Foxp3^+$ cells from 6 independently performed experiments were determined, each with spleen from one mouse (*N =13 $CREB^{fl/fl}$* and *N=12 $Foxp3^{cre}CREB^{fl/fl}$* mice), a two tailed unpaired t-test was used to test for significance. H) Statistical analysis of IL-10^+ cells within $Foxp3^+$ cells after treatment as in G). An unpaired, two tailed t-test was used to test for significance, each dot represents one animal and error bars SEM I) IL-10 in supernatants of $CD4^+CD25^-$ T cells after stimulation with anti-CD3/CD28 antibodies in the presence of 5 ng/ml TGF-β for five days measured by ELISA , an unpaired two- tailed t test was performed to test for significance, bars indicate mean and error bars SEM (*N = 6*). J)-L) Δ ct mRNA expression of cells after treatment as in G, each dot represents one animal and error bars SEM, two tailed unpaired t-tests were used to test for significance. M) Statistical analysis of Splenic $ST2^+$ cells within $CD4^+$ and $CD4^+CD25^+$ cells of *$CREB^{fl/fl}$* and *$Foxp3^{Cre}CREB^{fl/fl}$* mice. 3 independently performed experiments (*N = 10 $CREB^{fl/fl}$* and *N =11 $Foxp3^{cre}CREB^{fl/fl}$* mice), a two tailed unpaired t-test was used to test for significance, each dot represents one animal and error bars SEM. N) Representative density plot of M. O) N-fold *Crem* mRNA expression in splenic T_{regs} from from *$CREB^{fl/fl}$* and *$Foxp3^{cre}CREB^{fl/fl}$* mice (N = 3, male, 8-10 weeks old) cells analyzed by RT-qPCR. Bars indicate mean and error bars SEM.

Figure 5: Genome-wide chromatin accessibility of *CREB*$^{fl/fl}$ and *Foxp3*^{cre}*CREB*$^{fl/fl}$ mice. A) ATAC-seq footprinting analysis indicates decrease in TF activity for CREB1 and CREM upon CREB1 KO and increase in TF activity of NRF1 upon CREB KO. B) Example of genes with loss of chromatin accessibility upon CREB1 KO includes an alternative promoter of CREM (read peaks) and enhancer regions around SC-2/Il1nl1 (blue peaks). C) CD4^{+}CD25^{-} T cells were stimulated with anti-CD3/CD28 antibodies in the presence/absence of 5 ng/ml TGF-β for five days. Percentages of Foxp3^{+} cells from 6 independently performed experiments were determined, each with spleen from one mouse, *N* = 13 *CREB*$^{fl/fl}$, *N = 12 Foxp3*^{cre}*CREB*$^{fl/fl,}$ and *N = 3 Foxp3*^{cre}*CREB*$^{fl/fl}$*CREM*$^{-/-}$ mice, a two tailed unpaired t-test was used to test for significance, bars indicate mean and error bars SEM. 3 D) Statistical analysis of MFI of Foxp3 in *CCRE* (*N* = 13) and *Foxp3*^{cre}*CREB*$^{fl/fl}$ (N = 9) and *Foxp3*^{cre}*CREB*$^{fl/fl}$*CREM*$^{-/-}$ (*N* =3) CD4^{+}CD25^{+} T cells, bars indicate mean and error bars SEM, two tailed unpaired t-test was used to test for significance. E) Statistical analysis of ST2^{+} in CD4^{+} and CD4^{+}Foxp3^{+} cells in *CREB*$^{fl/fl}$ (*N* = 5) and *Foxp3*^{cre}*CREB*$^{fl/fl}$ (*N = 6*) and *Foxp3*^{cre}*CREB*$^{fl/fl}$*CREM*$^{-/-}$ (*N* =3) CD4^{+}CD25^{+} T cells, bars indicate mean and error bars SEM, two tailed unpaired t-test was used to test for significance. F) Statistical analysis of ST2+ in CD4+ and CD4+RFP+ cells in *Foxp3*^{cre}*ROSA*^{RFP} (*N = 5*) and *Foxp3*^{cre}*CREB*$^{fl/fl}$*ROSA*^{RFP} (*N = 5*) in spleen, bars indicate mean and error bars SEM, two tailed unpaired t-test was used to test for significance. G) Statistical analysis of ST2+ in CD4+ and CD4+RFP+ cells in *Foxp3*^{cre}*ROSA*^{RFP} (*N = 5*) and *Foxp3*^{cre}*CREB*$^{fl/fl}$*ROSA*^{RFP} (N = 5) in mesenteric lymph node, bars indicate mean and error bars SEM, two tailed unpaired t-test was used to test for significance. H) Statistical analysis of ST2+ in CD4+ and CD4+RFP+ cells in *Foxp3*^{cre}*ROSA*^{RFP} (*N = 4*) and *Foxp3*^{cre}*CREB*$^{fl/fl}$*ROSA*^{RFP} (*N = 4*) in thymus, bars indicate mean and error bars SEM, two tailed unpaired t-test was used to test for significance. I) Statistical analysis of ST2+ in CD4+ and CD4+RFP+ cells in *Foxp3*^{cre}*ROSA*^{RFP} (*N = 5*) and *Foxp3*^{cre}*CREB*$^{fl/fl}$*ROSA*^{RFP} (*N = 5*) in lung, bars indicate mean and error bars SEM, two tailed unpaired t-test was used to test for significance. J) Statistical analysis of ST2+ in CD3+ and CD3+RFP+ cells in *Foxp3*^{cre}*ROSA*^{RFP} (*N = 5*) and *Foxp3*^{cre}*CREB*$^{fl/fl}$*ROSA*^{RFP} (*N = 5*) in colon, bars indicate mean and error bars SEM, two tailed unpaired t-test was used to test for significance.

Figure 6: Foxp3 interacts with CREM and CREB

CD4+ T-cells were isolated and differentiated from splenocytes with 3 µg/ml anti-CD3 und anti-CD28 and 5 ng/ml TGF-β for 5 days and Co-IP was performed. A) Co-IP of Foxp3 and CREB and B) Co-IP of Foxp3 and CREM. Nuclear and cellular extracts were used directly and

nuclear lysates were subjected to Co-IP and detected by means of Western blot. Anti-Foxp3 antibody was used for the protein binding and anti -CREB or anti -CREM antibody for detection. The size was determined by means of a protein marker.

Figure 7: *Foxp3^{cre}Creb$^{fl/fl}$* CD4+ T cells induce only moderate inflammation in experimental colitis. Rag$^{-/-}$ mice were adoptively transferred with CD4^{+} wild-type cells (*CREB$^{fl/fl}$* CD4^{+}) or *Foxp3^{CRE}CREB$^{fl/fl}$* CD4^{+} T cells. Untreated Rag$^{-/-}$ mice were used as controls (K). Mice were weighed and sacrificed 5 weeks after transfer. (A) Body weight as a percent of starting weight. (B) Results of histological TJL (The Jackson Laboratory Score) scoring of colon sections (two independently performed experiments, *CREB$^{fl/fl}$* recipients N = 5, *Foxp3^{cre}CREB$_{fl/fl}$* recipients N = 6). C) Representative photomicrographs of hematoxylin and eosin (H&E)-stained colon sections imaged using a 10 x objective. D) Expression of inflammatory cytokines analyzed by RT-qPCR. Dots represent Δ ct values normalized to β-actin. Each dot represents one animal. (Ct levels are inversely proportional to the amount of target nucleic acid in the sample), two tailed unpaired t-tests were used to test for significance. E) Statistical analysis of IL-17^{+} cells within CD4^{+} cells in mLNs (three independently performed experiments, *CREB$^{fl/fl}$* recipients N = 9, *Foxp3^{cre}CREB$^{fl/fl}$* recipients N = 9), a two-tailed, unpaired t-test was used. F) Statistical analysis of IFN-γ^{+} cells within CD4^{+} cells in mLNs. (three independently performed experiments, *CREB$^{fl/fl}$* recipients *N = 11*, *Foxp3^{cre}CREB$^{fl/fl}$* recipients *N = 9*), two-tailed, unpaired t-test was used. G) Representative dot plots of E and F.

Figure 8: *Foxp3^{cre}CREB$^{fl/fl}$ROSA^{RFP}* CD4+ T cells induce only moderate inflammation in experimental colitis, while CD4+RFP+ cells expand in peripheral tissues. Rag$^{-/-}$ mice were adoptively transferred with CD4^{+} CD25^{-} wild-type cells (*Foxp^{cre}ROSA^{RFP}*CD4^{+}CD25^{-}) or *Foxp3^{cre}CREB$^{fl/lf}$ROSA^{RFP}* CD4^{+} CD25^{-} T cells. Mice were weighed and sacrificed 5 weeks after transfer. (A) Body weight as a percent of starting weight, two-tailed unpaired t-test were used to test for significance (*N = 5 Foxp^{cre}ROSA^{RFP}* and *N = 5 Foxp3^{cre}CREB$^{fl/lf}$ROSA^{RFP}* recipient mice were analyzed in 1 independently performed experiment). (B) Representative Flow cytometry gated on CD4 and RFP in splenocytes. Percentages of CD45^{+}CD3^{+}CD4^{+}RFP^{+} cells in C) Spleen, D) mLNs, E) Colon, F) Lung, and G) Liver, two-tailed, unpaired t-test was used.

Figure 9: Reduced colitis in *Foxp3^{CRE}CREB$^{fl/fl}$* CD4^{+} T cell recipients depends on IL-10 signaling. Rag2$^{-/-}$ mice were adoptively transferred with CD4^{+} wild-type cells (WT CD4^{+}) or *Foxp3^{cre}CREB$^{fl/fl}$* CD4^{+} T cells. Mice were either treated with an anti-IL10R antibody or an isotype control. (A) Body weight as a percent of starting weight, Bars indicate mean and error bars SEM (*N=5* animals in each group, a two-tailed unpaired t-test was used, two independently performed experiments). B) Representative photomicrographs of a hematoxylin and eosin (H&E)-stained colon section from *CREB$^{fl/fl}$* and *Foxp3^{cre}CREB$^{fl/fl}$* CD4^{+} T cell recipients, that were treated with anti-IL10R, imaged using a 10x objective. C) Results of histological JLS (The Jackson Laboratory Scoring) score of colon sections (two independently performed experiments with overall *N=5* mice in each group, two-independently performed experiments, a two tailed Mann Whitney test was used to test for significance). D) Body weight as a percent of starting weight, Bars indicate mean and error bars SEM (Wild type *N=3 and Foxp3^{cre}CREB$^{fl/fl}$ CREM-/- N = 4* animals, a two-tailed unpaired t-test was used, one independently performed experiment). E) Results of histological JLS (The Jackson Laboratory Scoring) score of colon sections (Wild type mice *N=4 and Foxp3^{cre}CREB$^{fl/fl}$ CREM-/- N = 6* animals, two-independently performed experiments, a two-tailed unpaired t-test was used to test for significance). F) Statistical analysis of CD4+ T-cell frequencies (Wild type *N=3 and Foxp3^{cre}CREB$^{fl/fl}$ CREM-/- N = 4* animals, a two-tailed unpaired t-test was used, one independently performed experiment). G) Statistical analysis of IFN-γ^{+} with in CD4+ cells (Wild type *N=3 and Foxp3^{cre}CREB$^{fl/fl}$ CREM-/- N = 4* animals, a two-tailed unpaired t-test was used, one independently performed experiment). H) Statistical analysis of IL-10^{+} with in CD4+ cells (Wild type *N=3 and Foxp3^{cre}CREB$^{fl/fl}$ CREM-/- N = 4* animals, a two-tailed unpaired t-test was used, one independently performed experiment).

Fig. 10: *Foxp3^{CRE}CREB$^{fl/fl}$* mice display enhanced type 2 immune responses. A) IgE antibodies in the serum of mice were determined by ELISA. C) OVA-induced asthma (6-8 weeks old, age-matched) B-D) Lung function parameters in sensitized *CREB$^{fl/fl}$* and *Foxp3^{cre}CREB$^{fl/fl}$* mice were measured using the flexiVent system (n=7 in both groups). Total lung resistance Rrs (B), elastance E (C) and tissue damping H (D). E) Statistical analysis of splenic percentages of ST2^{+} cells in CD45^{+}CD4^{+}Foxp3^{+} in *CREB$^{fl/fl}$* and *Foxp3^{cre}CREB$^{fl/fl}$* mice, a two tailed, unpaired t-test was used, each plot represents on mouse. F) Statistical analysis of percentages ST2^{+} cells in CD45^{+}CD4^{+}Foxp3^{+} in *CREB$^{fl/fl}$* and *Foxp3^{cre}CREB$^{fl/fl}$* mice in the BAL, a two tailed, unpaired t-test was used, each plot represents on mouse.

A

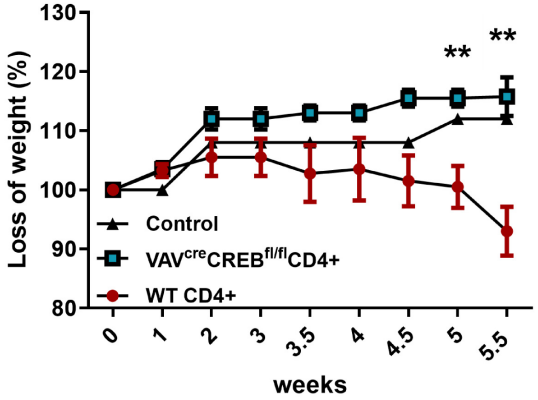
130
120
110
100
90
80
Loss of weight (%)
**
**
Control
VAV^{cre}CREB$^{fl/fl}$CD4+
WT CD4+
0
1
2
3
3.5
4
4.5
5
5.5
weeks

B

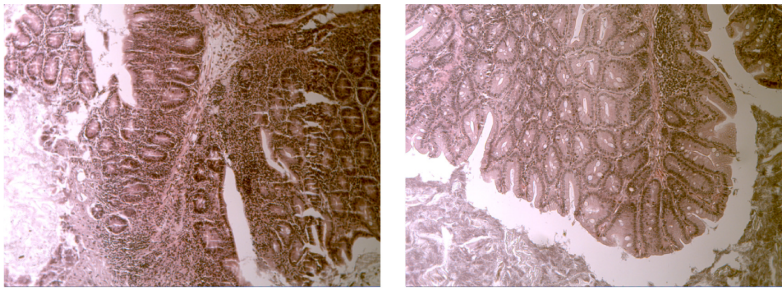
WT
VAV^{cre}CREB$^{fl/fl}$

C

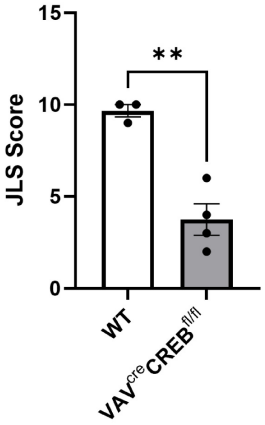
15
10
5
0
JLS Score
**
WT
VAV^{cre}CREB$^{fl/fl}$

D

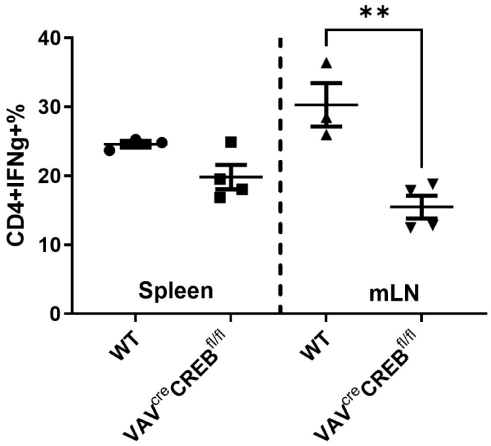
40
30
20
10
0
CD4+IFNg+%
**
Spleen
mLN
WT
VAV^{cre}CREB$^{fl/fl}$
WT
VAV^{cre}CREB$^{fl/fl}$

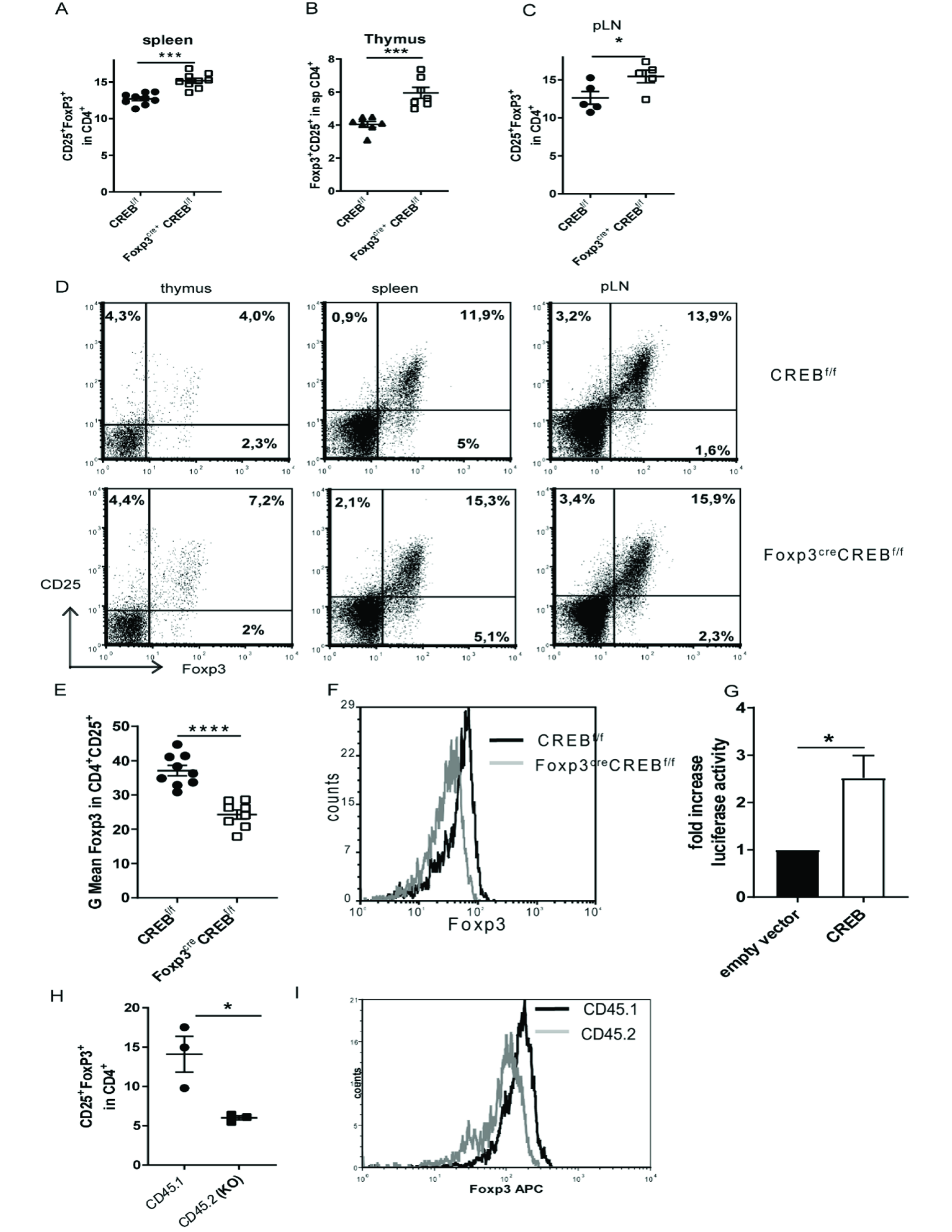
A
spleen
***
CD25+FoxP3+ in CD4+
CREBf/f
Foxp3cre+ CREBf/f
B
Thymus
***
Foxp3+CD25+ in sp CD4+
C
pLN
*
D
thymus
spleen
pLN
4,3%
4,0%
2,3%
0,9%
11,9%
5%
3,2%
13,9%
1,6%
CREBf/f
4,4%
7,2%
2%
2,1%
15,3%
5,1%
3,4%
15,9%
2,3%
Foxp3creCREBf/f
CD25
Foxp3
E
****
G Mean Foxp3 in CD4+CD25+
CREBf/f
Foxp3cre CREBf/f
F
counts
CREBf/f
Foxp3creCREBf/f
Foxp3
G
*
fold increase luciferase activity
empty vector
CREB
H
*
CD25+FoxP3+ in CD4+
CD45.1
CD45.2 (KO)
I
CD45.1
CD45.2
counts
Foxp3 APC

A

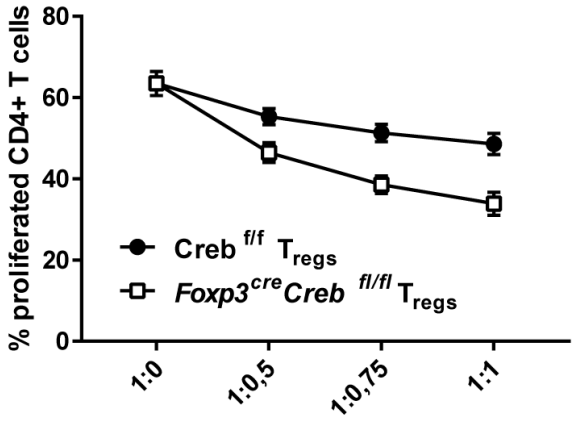
% proliferated CD4+ T cells
80
60
40
20
0
Creb f/f Tregs
Foxp3cre Creb fl/fl Tregs
1:0
1:0,5
1:0,75
1:1

B

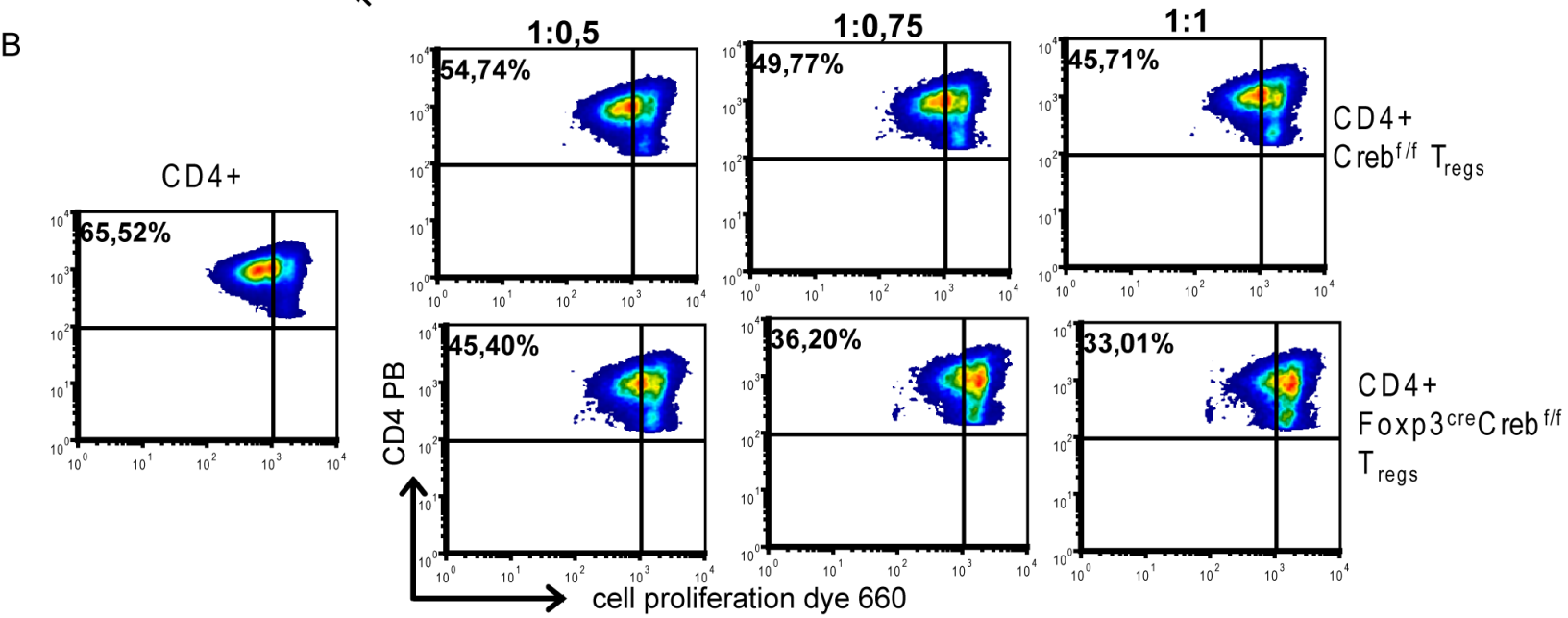
1:0,5
1:0,75
1:1
CD4+
65,52%
54,74%
49,77%
45,71%
CD4+ Creb f/f Tregs
45,40%
36,20%
33,01%
CD4+ Foxp3cre Creb f/f Tregs
CD4 PB
cell proliferation dye 660

C

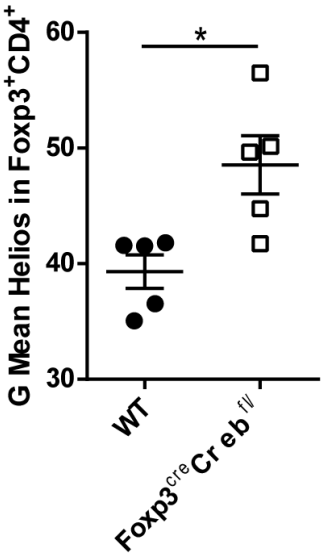
G Mean Helios in Foxp3+CD4+
60
50
40
30
*
WT
Foxp3cre Creb fl/

D

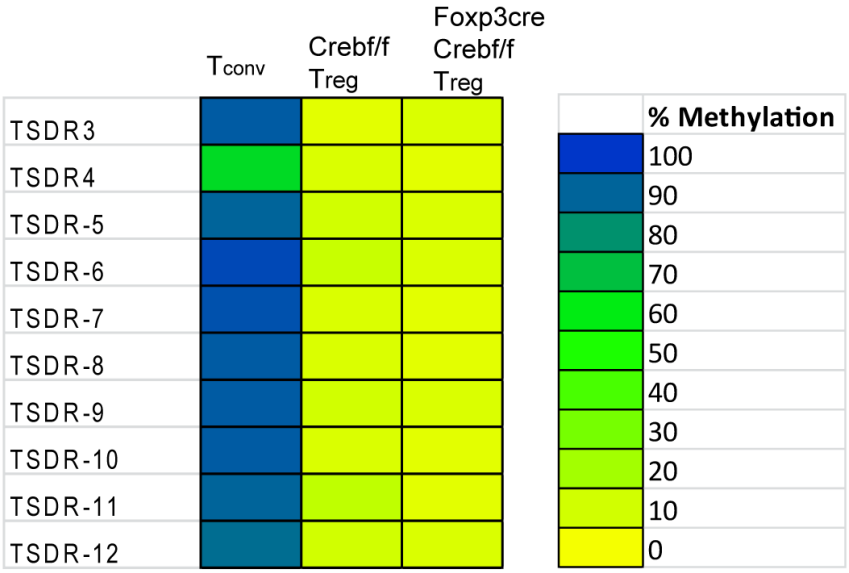
Tconv
Crebf/f Treg
Foxp3cre Crebf/f Treg
TSDR3
TSDR4
TSDR-5
TSDR-6
TSDR-7
TSDR-8
TSDR-9
TSDR-10
TSDR-11
TSDR-12
% Methylation
100
90
80
70
60
50
40
30
20
10
0

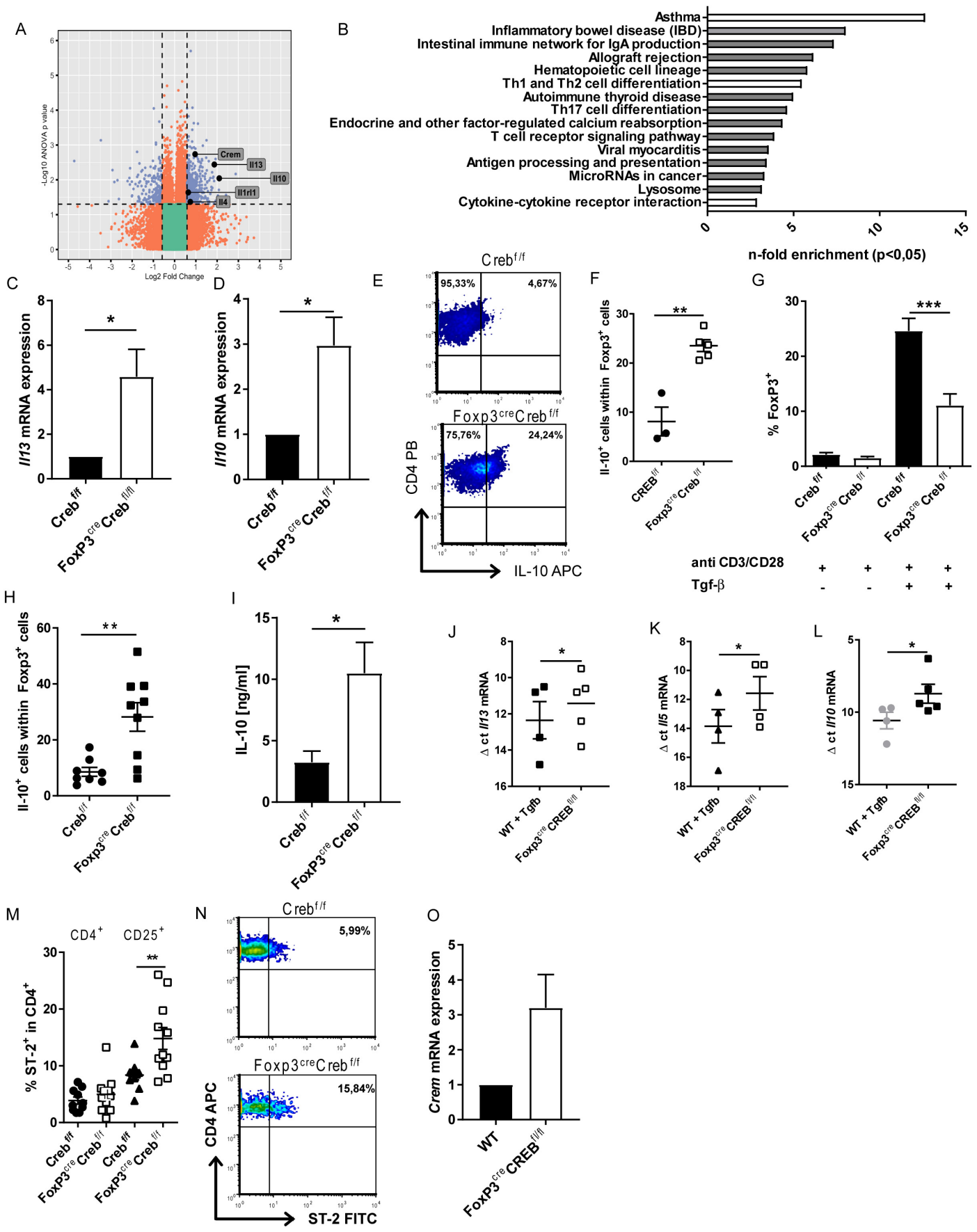
A
-Log10 ANOVA p value
Log2 Fold Change
Crem
Il13
Il10
Il1rl1
Il4
B
Asthma
Inflammatory bowel disease (IBD)
Intestinal immune network for IgA production
Allograft rejection
Hematopoietic cell lineage
Th1 and Th2 cell differentiation
Autoimmune thyroid disease
Th17 cell differentiation
Endocrine and other factor-regulated calcium reabsorption
T cell receptor signaling pathway
Viral myocarditis
Antigen processing and presentation
MicroRNAs in cancer
Lysosome
Cytokine-cytokine receptor interaction
n-fold enrichment (p<0,05)
C
Il13 mRNA expression
Creb f/f
FoxP3cre Creb fl/fl
D
Il10 mRNA expression
Creb f/f
FoxP3cre Creb f/f
E
Creb f/f
95,33%
4,67%
Foxp3cre Creb f/f
75,76%
24,24%
CD4 PB
IL-10 APC
F
Il-10+ cells within Foxp3+ cells
CREB f/f
Foxp3cre Creb f/f
G
% FoxP3+
Creb f/f
Foxp3cre Creb f/f
Creb f/f
Foxp3cre Creb f/f
anti CD3/CD28
Tgf-β
H
Il-10+ cells within Foxp3+ cells
Creb f/f
Foxp3cre Creb f/f
I
IL-10 [ng/ml]
Creb f/f
FoxP3cre Creb f/f
J
Δ ct Il13 mRNA
WT + Tgfb
Foxp3cre CREB fl/fl
K
Δ ct Il5 mRNA
WT + Tgfb
Foxp3cre CREB fl/fl
L
Δ ct Il10 mRNA
WT + Tgfb
Foxp3cre CREB fl/fl
M
CD4+
CD25+
% ST-2+ in CD4+
Creb f/f
FoxP3cre Creb f/f
Creb f/f
FoxP3cre Creb f/f
N
Creb f/f
5,99%
Foxp3cre Creb f/f
15,84%
CD4 APC
ST-2 FITC
O
Crem mRNA expression
WT
FoxP3cre CREB fl/fl

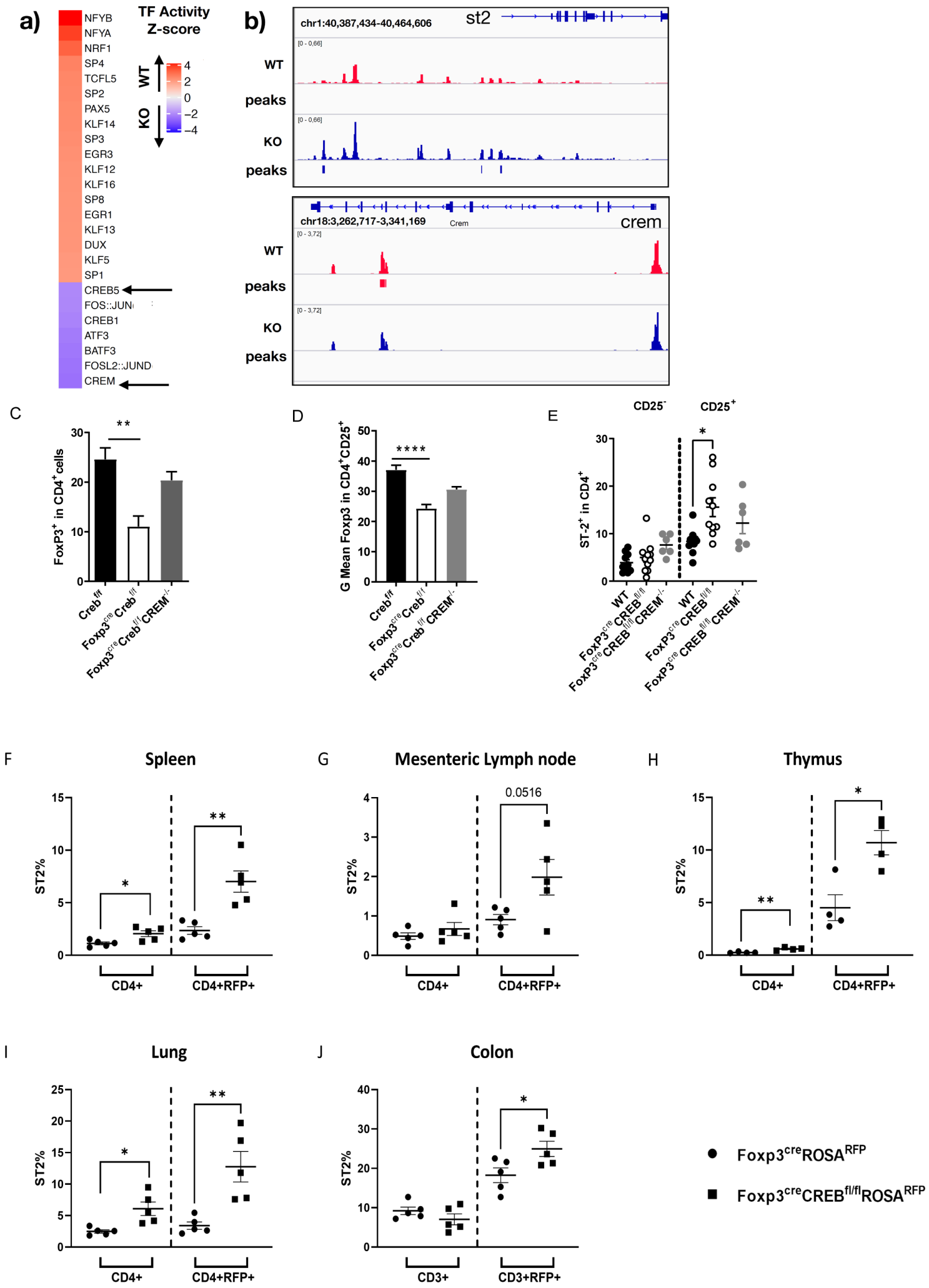
a)
TF Activity Z-score
NFYB
NFYA
NRF1
SP4
TCFL5
SP2
PAX5
KLF14
SP3
EGR3
KLF12
KLF16
SP8
EGR1
KLF13
DUX
KLF5
SP1
CREB5
FOS::JUN
CREB1
ATF3
BATF3
FOSL2::JUND
CREM
WT
KO
4
2
0
−2
−4
b)
chr1:40,387,434-40,464,606
st2
WT
peaks
KO
peaks
chr18:3,262,717-3,341,169
Crem
crem
C
FoxP3+ in CD4+cells
Creb f/f
Foxp3cre Creb f/f
Foxp3cre Creb f/f CREM-/-
D
G Mean Foxp3 in CD4+CD25+
E
CD25-
CD25+
ST-2+ in CD4+
WT
FoxP3cre CREB fl/fl
FoxP3cre CREB fl/fl CREM-/-
F
Spleen
G
Mesenteric Lymph node
0.0516
H
Thymus
ST2%
CD4+
CD4+RFP+
I
Lung
J
Colon
CD3+
CD3+RFP+
Foxp3creROSARFP
Foxp3creCREBfl/flROSARFP

A

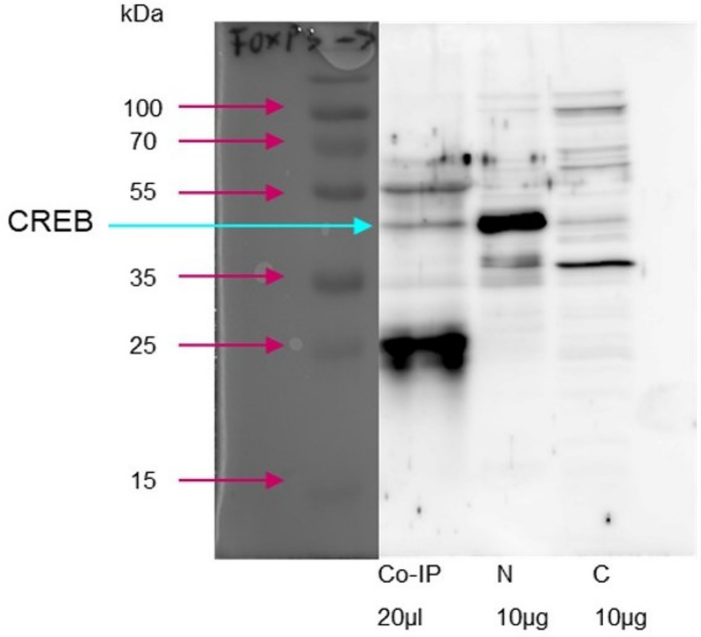
kDa
100
70
55
CREB
35
25
15
Co-IP
20µl
N
10µg
C
10µg

B

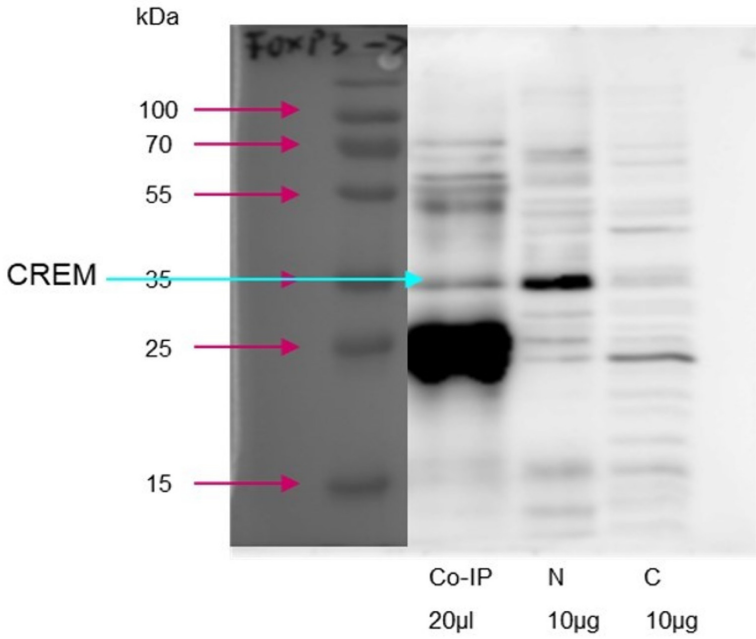
kDa
100
70
55
CREM
35
25
15
Co-IP
20µl
N
10µg
C
10µg

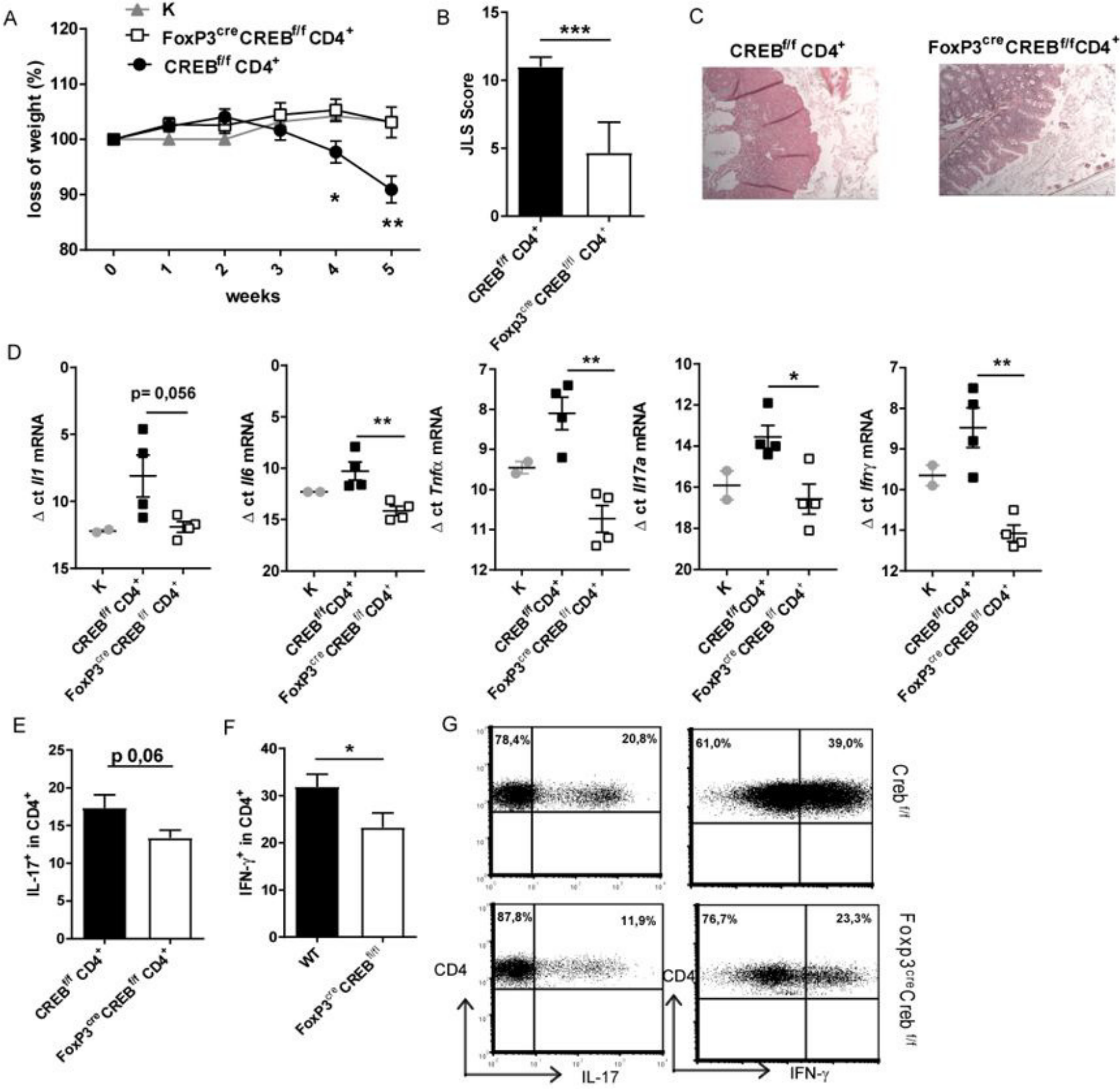
A
K
FoxP3cre CREBf/f CD4+
CREBf/f CD4+
loss of weight (%)
weeks
B
JLS Score
***
CREBf/f CD4+
Foxp3cre CREBf/f CD4+
C
CREBf/f CD4+
FoxP3cre CREBf/f CD4+
D
p= 0,056
Δ ct Il1 mRNA
Δ ct Il6 mRNA
Δ ct Tnfα mRNA
Δ ct Il17a mRNA
Δ ct Ifnγ mRNA
K
CREBf/f CD4+
FoxP3cre CREBf/f CD4+
E
p 0,06
IL-17+ in CD4+
CREBf/f CD4+
FoxP3cre CREBf/f CD4+
F
IFN-γ+ in CD4+
WT
FoxP3cre CREBf/f
G
78,4%
20,8%
61,0%
39,0%
87,8%
11,9%
76,7%
23,3%
Creb f/f
Foxp3cre Creb f/f
CD4
IL-17
IFN-γ

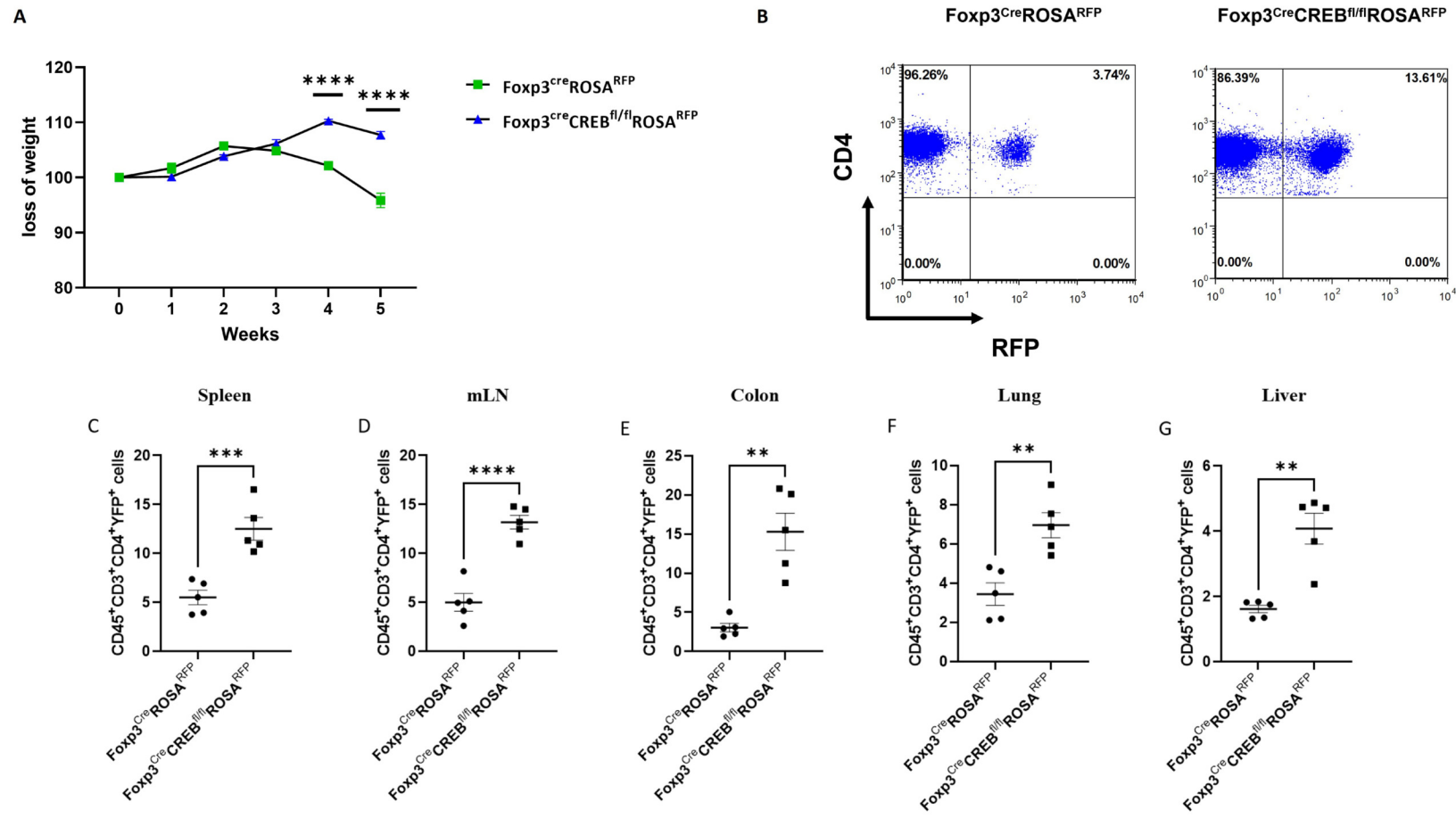
A
B
Foxp3CreROSARFP
Foxp3CreCREBfl/flROSARFP
loss of weight
Weeks
****
****
96.26%
3.74%
0.00%
0.00%
86.39%
13.61%
0.00%
0.00%
CD4
RFP
Spleen
mLN
Colon
Lung
Liver
C
D
E
F
G
CD45+CD3+CD4+YFP+ cells
***
****
**
**
**

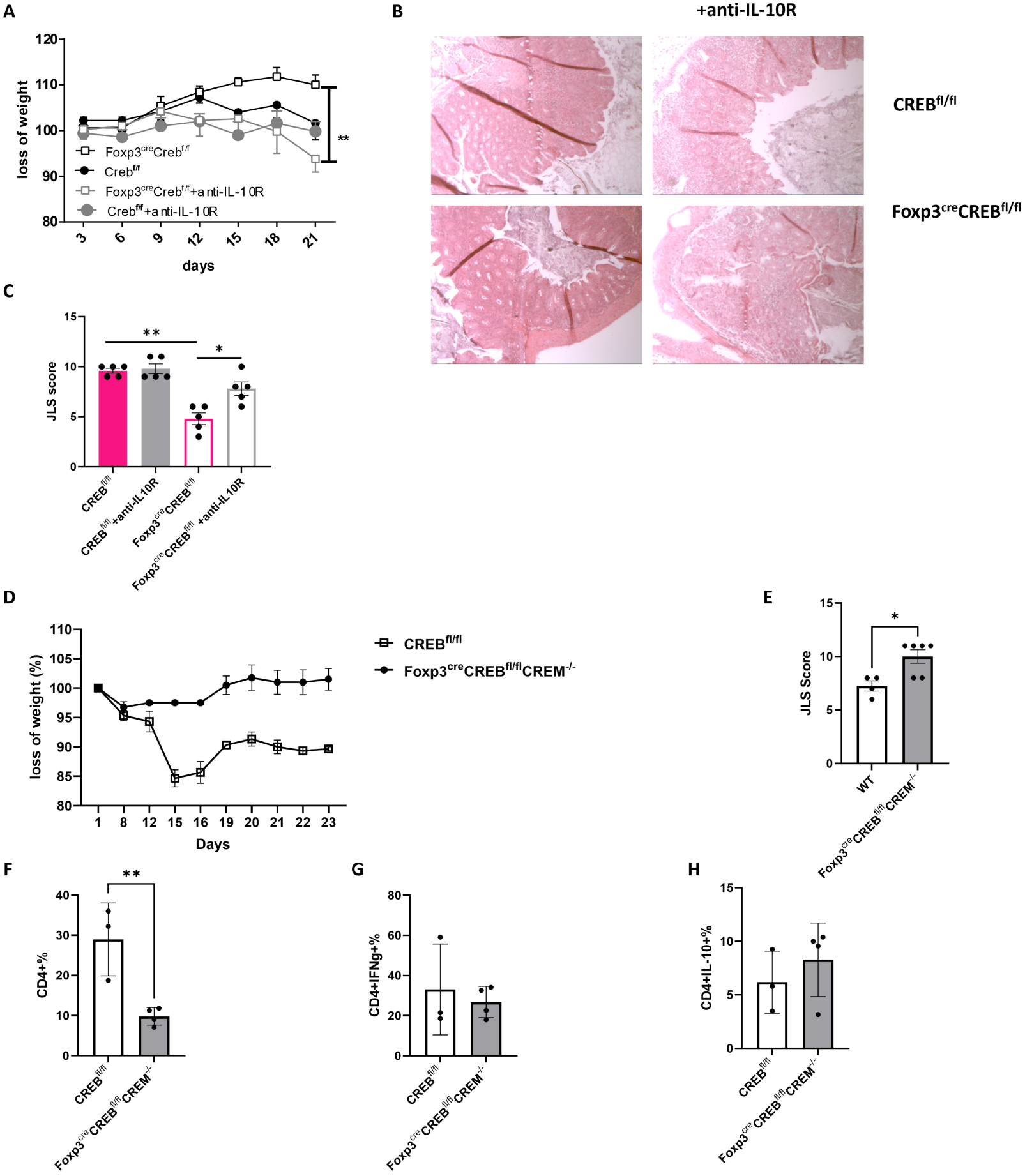
A
loss of weight
days
Foxp3cre Creb f/f
Creb f/f
Foxp3cre Creb f/f +anti-IL-10R
Creb f/f +anti-IL-10R
**
B
+anti-IL-10R
CREBfl/fl
Foxp3creCREBfl/fl
C
JLS score
**
*
CREBfl/fl
CREBfl/fl +anti-IL10R
Foxp3creCREBfl/fl
Foxp3creCREBfl/fl +anti-IL10R
D
loss of weight (%)
Days
CREBfl/fl
Foxp3creCREBfl/flCREM-/-
E
JLS Score
*
WT
Foxp3creCREBfl/flCREM-/-
F
CD4+%
**
CREBfl/fl
Foxp3creCREBfl/flCREM-/-
G
CD4+IFNg+%
CREBfl/fl
Foxp3creCREBfl/flCREM-/-
H
CD4+IL-10+%
CREBfl/fl
Foxp3creCREBfl/flCREM-/-

A

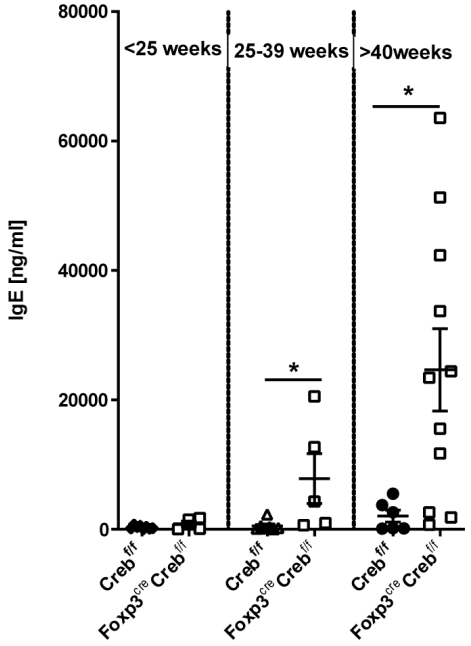
80000
60000
40000
20000
0
IgE [ng/ml]
<25 weeks
25-39 weeks
>40weeks
*
*
Creb f/f
Foxp3cre Creb f/f
Creb f/f
Foxp3cre Creb f/f
Creb f/f
Foxp3cre Creb f/f

B

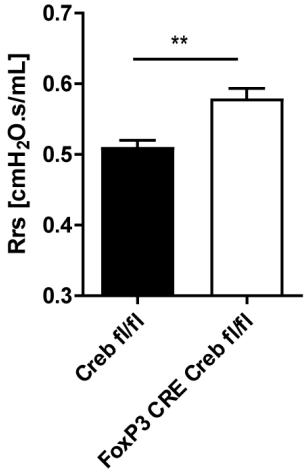
0.7
0.6
0.5
0.4
0.3
Rrs [cmH2O.s/mL]
**
Creb fl/fl
FoxP3 CRE Creb fl/fl

C

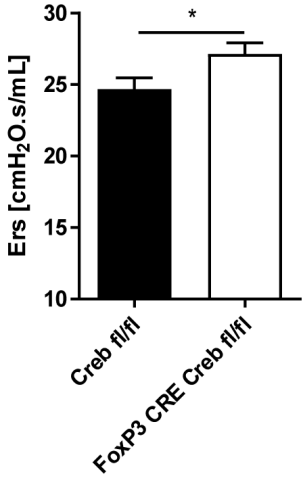
30
25
20
15
10
Ers [cmH2O.s/mL]
*
Creb fl/fl
FoxP3 CRE Creb fl/fl

D

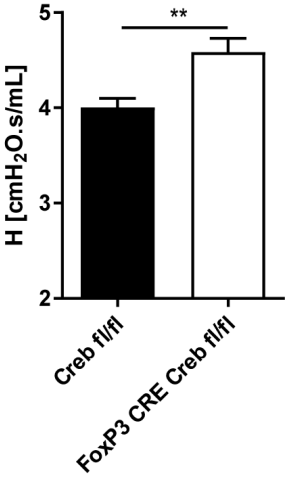
5
4
3
2
H [cmH2O.s/mL]
**
Creb fl/fl
FoxP3 CRE Creb fl/fl

E

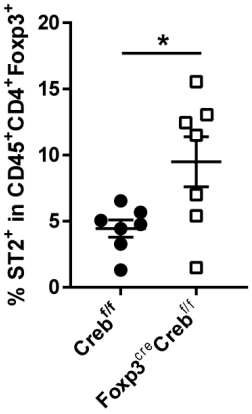
20
15
10
5
0
% ST2+ in CD45+CD4+Foxp3+
*
Creb f/f
Foxp3cre Creb f/f

F

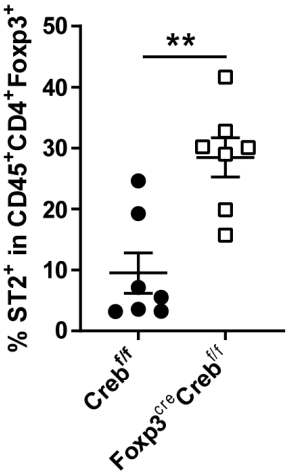
50
40
30
20
10
0
% ST2+ in CD45+CD4+Foxp3+
**
Creb f/f
Foxp3cre Creb f/f